9. MEASURES OF SHAKING TABLE PERFORMANCE

9.1. INTRODUCTION

In the case of a newly assembled shaking table, like the one at the UPRM Civil Engineering Department, it is necessary an evaluation of the accuracy of the input motion reproduction by the table. Furthermore, it is necessary to conduct a complete study of the table behavior in order to determine the calibration parameters for which the table can provide the best accuracy in earthquake reproduction [9].

9.2. EXPERIMENTAL TESTS FOR DETERMINATION OF SHAKING TABLE PERFORMANCE

A comprehensive investigation of table performance should use several types of input motions. The following discussion on the types of input motion is based on Mills [3]. The different types of input motion should include the following:

1. A Square wave
2. A Sinusoidal wave
3. White noise, modified by high and low-pass filtering
4. Actual earthquake time histories, with various model scaling factors

Each form of input motion provides a specific insight into the shake table response characteristics. Also, each type of test should be carried out for different parameters such as frequency, amplitude and payload conditions (bare table, rigid payload and flexible SDOF/MDOF payload).

An initial subjective determination of the quality of shake table reproduction was obtained by carrying out preliminary experimental tests. The preliminary tests involved the following input motions:

1. Square wave - provided information on the bare (unloaded) shaking table stability and rate of response.
2. Sinusoidal wave - provided the amplitude spectra envelope of the shaking table response and the frequency performance limitations.

These tests were carried out only in the bare table condition.

9.3. CALIBRATION PARAMETERS

The right calibration parameters or control gain settings for the different shake table payload conditions are found by a process called tuning. Tuning is discussed on the MTS manual titled “Controller Installation & Calibration” and the following discussion is based on this manual. Tuning affects the response and stability of the servo-control loop. Proper tuning improves the performance of the system by reducing error and phase lag [21]. Figure 9.1 illustrates this concept.

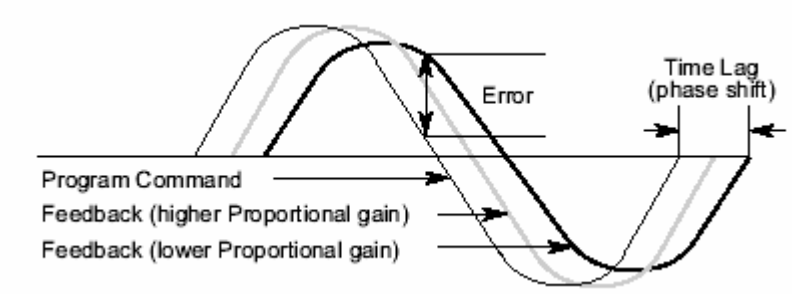

Figure 9.1 Definitions of Error and Phase Lag [21].

A control mode uses a program command and sensor feedback to control the servovalve [21]. For the purpose of tuning our system we utilized displacement control. This control mode uses the LVDT on the actuator as feedback signal. The TestStarAP controller uses a group of gain controls – proportional, integral, derivative and feed forward gain. These controls are called PIDF [21]. One does not need to use all of the

controls to properly tune a system. In fact, most testing can be accomplished with just proportional gain adjustment [21]. Proportional gain was used during our tests to tune the system. The five available gain controls have different functions.

9.3.1. PROPORTIONAL GAIN (P)

Proportional gain introduces a control factor that is proportional to the error signal. Proportional gain increases system response by increasing the effect of the error signal on the servovalve. Figure 9.2 shows the effects of proportional gain.

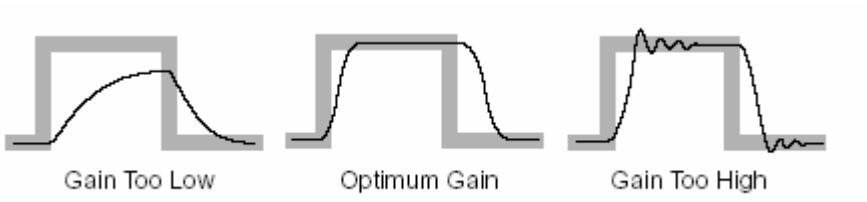

Figure 9.2 Effects of Proportional Gain on Sensor Feedback [21].

As proportional gain increases, the error decreases and the feedback signal tracks the command signal more closely. Too much proportional gain can cause the system to become unstable. In the other direction, too little proportional gain can cause the system to become sluggish. The MTS rule of thumb for proportional gain is to adjust gain as high as it will go without going unstable.

9.3.2. INTEGRAL GAIN (I)

Integral gain introduces “an integral of the error signal” that gradually, over time, increases the low-frequency response of the servovalve command. Integral gain maintains the mean level at high-frequency operation. Figure 9.3 shows the effects of integral gain. Higher integral gain settings increase system response. Too much integral

gain can cause a slow oscillation (hunting). The MTS rule of thumb is to set the integral gain to 10% of the proportional gain setting.

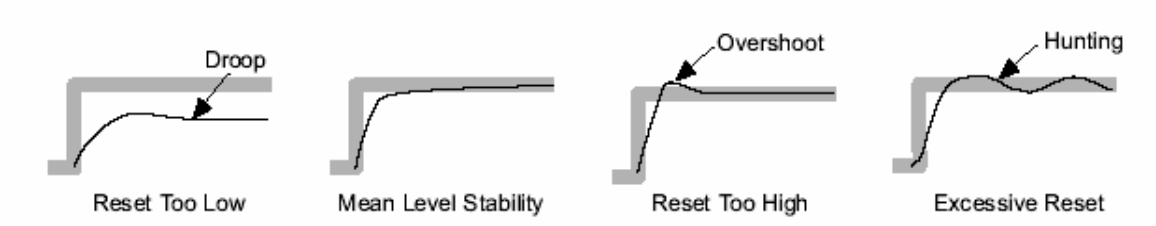

Figure 9.3 Effects of Integral Gain on Sensor Feedback [21].

9.3.3. DERIVATIVE GAIN (D)

It introduces a "derivative of the feedback signal". This means it anticipates the rate of change of the feedback and slows the system response at high rates of change. It reduces ringing, provides stability and reduces noise at higher proportional gain settings. Too much derivative gain can create instability at high frequencies, and way too much gain may cause a ringing or screeching sound. Too little derivative gain can make a rumbling sound. The correct amount of derivative gain results in the system running quietly. Figure 9.4 shows the effect of derivative gain.

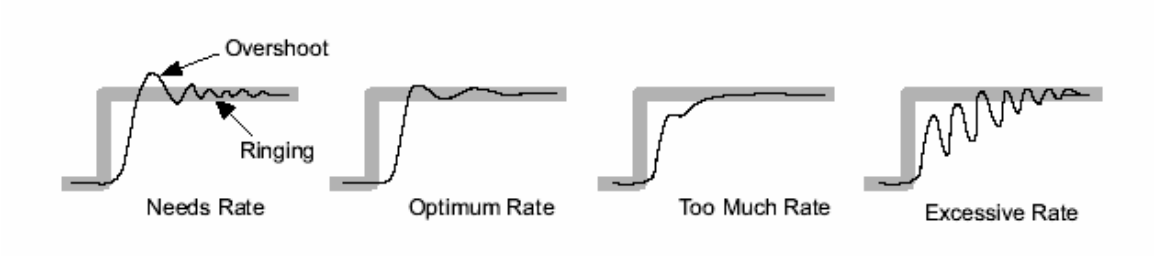

Figure 9.4 Effects of Derivative Gain on Sensor Feedback [21].

9.3.4. FEED FORWARD GAIN (F)

Feed forward gain is like derivative gain except that it introduces a derivative of the command signal. It anticipates how much valve opening is needed to reach the required response and adds that to the valve command – like compensating for phase lag. Feed

forward gain helps the servo-control loop to react quickly to an abrupt change in the command. Figure 9.5 shows the effect of feed forward gain.

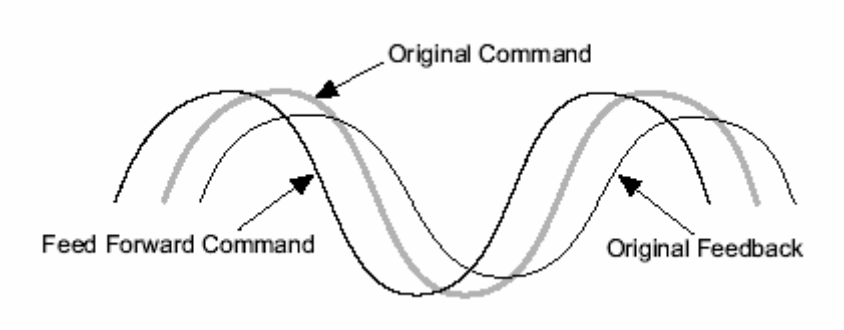

Figure 9.5 Effects of Feed Forward Gain on Sensor Feedback [21].

9.3.5. TUNING PROGRAM

The purpose of a tuning program is to produce a command that reflects the most demanding system response expected from a test. Square and ramp waveforms are preferred for initial tuning due to the fact that these waveforms have abrupt changes and excite the system at frequencies likely to be unstable with excessive gain. Final tuning can be done with the actual program for the test. MTS uses for a typical tuning program a low-amplitude (5% to 10% command), low-frequency (1 Hz to 2 Hz) square waveform [21].

For the purpose of obtaining the gain settings we utilize the square waveform and the sinusoidal waveform.

9.4. SQUARE WAVE

Shake table rate of response and stability can be investigated using square wave input [3]. The sensitivity settings for optimum table response can be found with this input motion. Figure 9.6 shows the effects of sensitivity on a square waveform.

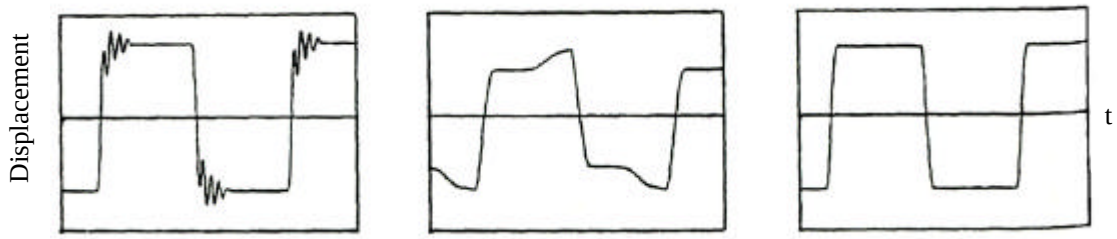

Figure 9.6 Effects of Sensitivity on a Square Waveform [3].

As seen from Figure 9.6, too much sensitivity can cause the system to become unstable as shown by the oscillations. On the other hand, too low sensitivity will cause a lack of ability to track the command signal. This characteristic should be investigated for various amplitudes and frequencies [3].

We used a single frequency and single amplitude for our tests to find the gain settings. For our tuning program, MTS technician Brad Schroenghamer recommended to use a square waveform of 0.1 Hz and amplitude of 5% of full range, which is ± 0.3175 cm (±0.125 in). For tracking the waveform we used the scope that comes with TestStarAP controller software. Figure 9.7 shows P-gain (K_P) tuning for our system.

It can be seen that as we increase the K_P the feedback signal (blue curve) tracks the command signal (red curve) more closely. Utilizing MTS criteria for K_P tuning, we can see some oscillation with K_P = 2.5, marked with the two circles. Figure 9.8 shows a close-up of the oscillations at K_P = 2.5. Therefore, the correct K_P is a number between 2.0 and 2.5. Figure 9.9 shows the K_P between 2.0 and 2.5. Figure 9.9 illustrates that the value of K_P before oscillation is K_P =2.4.

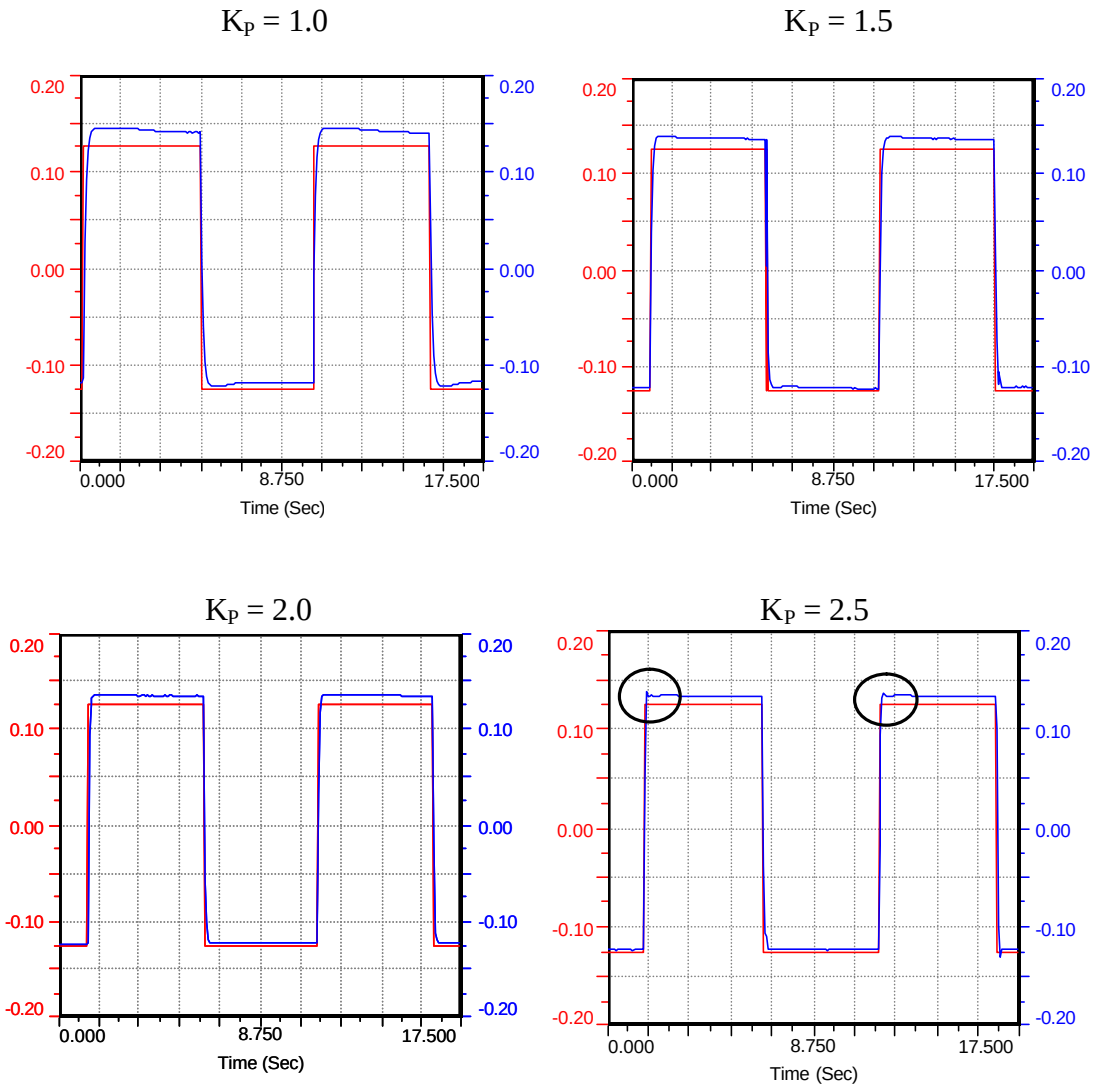

Figure 9.7 P-Gain (K_P) Tuning for a Square Wave.

Figure 9.10 shows the effect of the I-gain (K_I) on the waveform with K_P =2.4. It can be seen that the feedback signal tracks the command more closely, due to the effect of the K_I gain. We used K_I=0.250 for Figure 9.10 which is approximately 10% of the K_P =2.4 recommended by MTS. We conclude that for this tuning program the right control gain settings are K_P =2.4 and K_I=0.250.

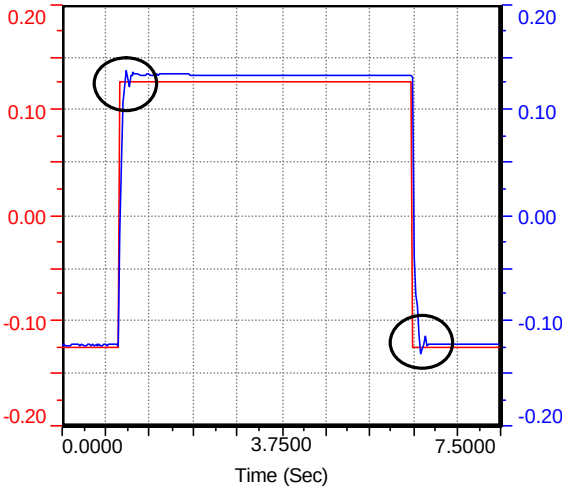

Figure 9.8 Close-Up of Oscillations at K_P =2.5.

K_P = 2.1

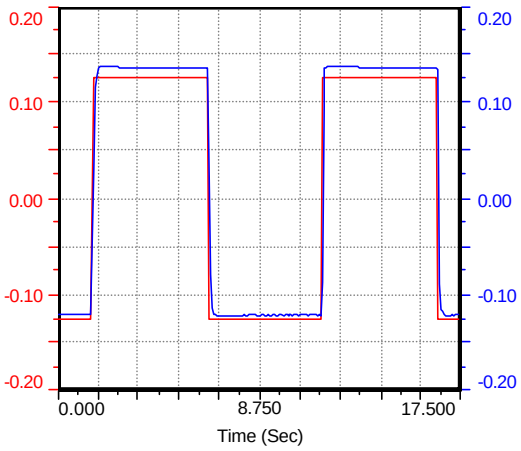

K_P = 2.2

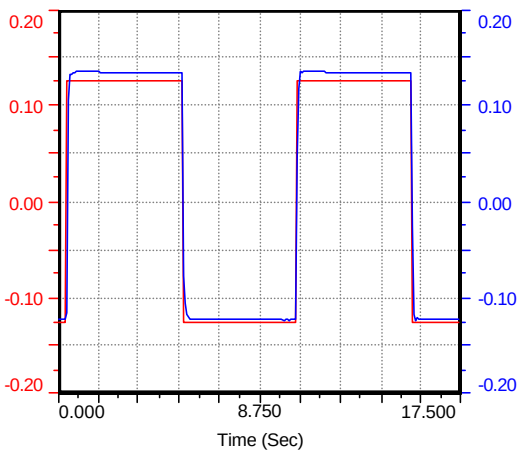

K_P = 2.3

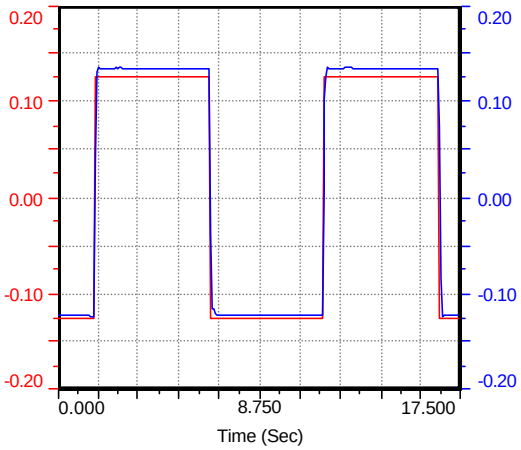

K_P = 2.4

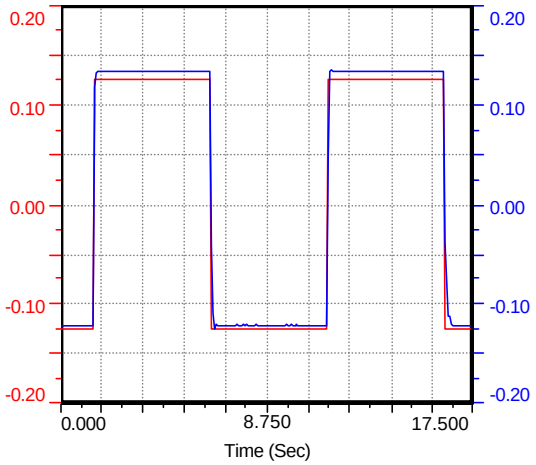

Figure 9.9 Scope Graphics for K_P = 2.1 to 2.4.

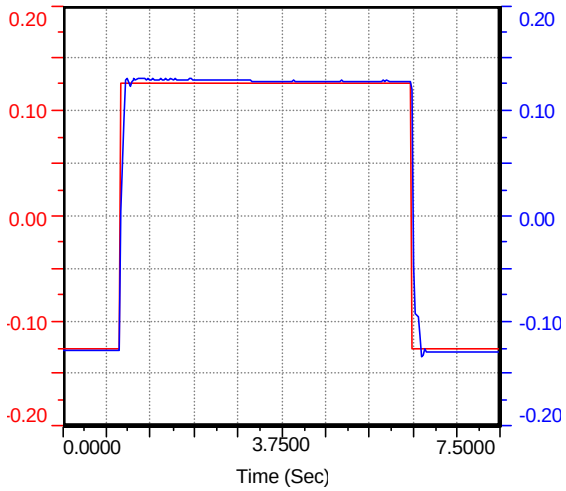

Figure 9.10 Effect of K_I on the Waveform.

9.5. SINUSOIDAL WAVE

9.5.1. COMPARISON OF INPUT/RESPONSE AMPLITUDE

An initial test would involve comparison of input amplitude to response amplitude at various frequencies of motion [3]. We used frequencies from 1.0 Hz to 18.0 Hz and single amplitude for our tests to find the gain settings. For our tuning program, MTS technician Brad Schroenghamer recommended to use the sine waveform of different frequencies and amplitude of 10% of full range, which is ± 0.635 cm (±0.250 in). For tracking the waveform we used the scope that comes with TestStarAP controller software. We also used a time meter that gave timed peak/valley feedback data to calculate error from command signal. Figure 9.11 shows the command error (peak) vs. P-gain (K_P) tuning for 1.0 to 10.0 Hz. Figure 9.12 shows the command error (valley) vs. P-gain (K_P) tuning for 1.0 to 10.0 Hz. From the Figures 9.11 and 9.12, it can be seen that from 1.0 to 6.0 Hz the error diminishes greatly as we increase the K_P. Also, we noticed

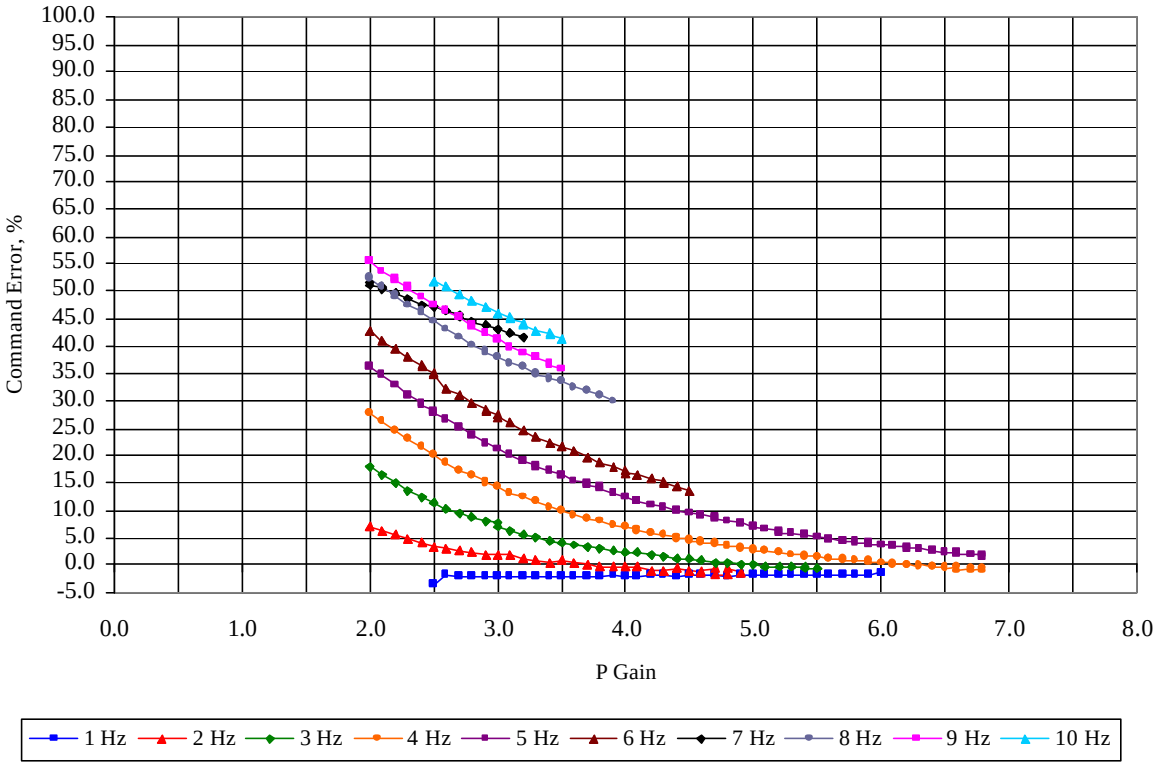

Figure 9.11 Command Error (peak) vs. P-gain (K_P) Tuning for 1.0 to 10.0 Hz.

that as the frequency increases the K_P needed to decrease the error increases. From K_P = 4.5 to 6.0 the peak error goes from 15% for 6.0 Hz to 5% for 5.0 Hz.

For the higher frequencies, from 7.0 to 10.0 Hz, the highest K_P goes from 3.5 to 3.9 and a peak error that goes from 50% to 40% for 10.0 Hz

From K_P = 4.5 to 6.0 the valley error goes from 20% for 6.0 Hz to 10% for 6.0 Hz. For the higher frequencies, from 7.0 to 10.0 Hz, the highest K_P goes from 3.5 to 3.9 and a valley error that goes from 60% to 50% for 10.0 Hz. In these frequencies we did not go higher with the K_P because some kind instability was showing in the system. It is recommended that in future tests in these frequencies to go higher with the K_P until the system goes almost unstable.

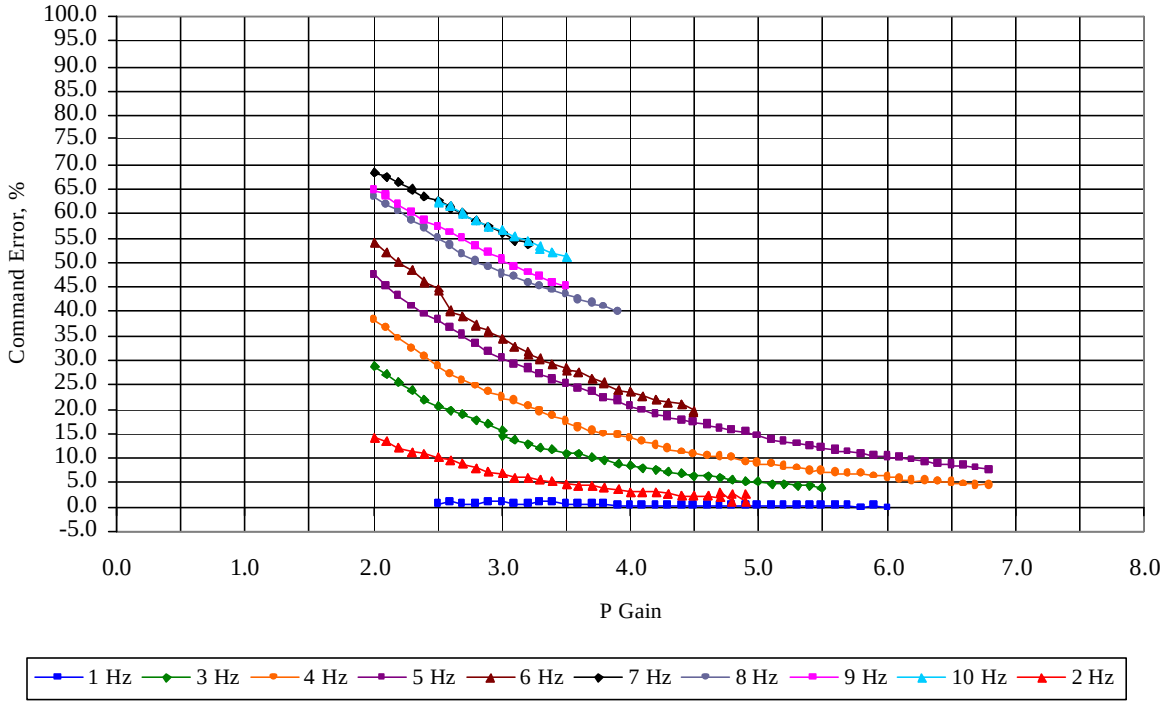

Figure 9.12 Command Error (valley) vs. P-gain (K_P) Tuning for 1.0 to 10.0 Hz.

We also tested the system for higher frequencies. We tested from 11.0 Hz to 18.0 Hz, at single amplitude also of 10% of full range that is ± 0.635 cm (±0.250 in). For tracking the waveform we used the scope that comes with TestStarAP controller software, also. To calculate the error from the command signal, we used the data from each test saved by the Data Acquisition System Software, DasyLab. Figure 9.13 shows the command error (peak) vs. P-gain (K_P) tuning for 11.0 to 18.0 Hz. Figure 9.14 shows the command error (valley) vs. P-gain (K_P) tuning for 11.0 to 18.0 Hz. According to Figure 9.13 the peak command error increased as the frequency increased. Also, we noticed that the error decreased almost linearly with K_P and the error decreased more slowly than for the lower frequencies (1 to 10 Hz). In addition, we noticed that some frequencies are grouped together. The lowest peak command error is 40% for 11.0 Hz at K_P = 4.0. The highest peak command error is 85% for 16, 17 and 18 Hz at K_P = 2.0.

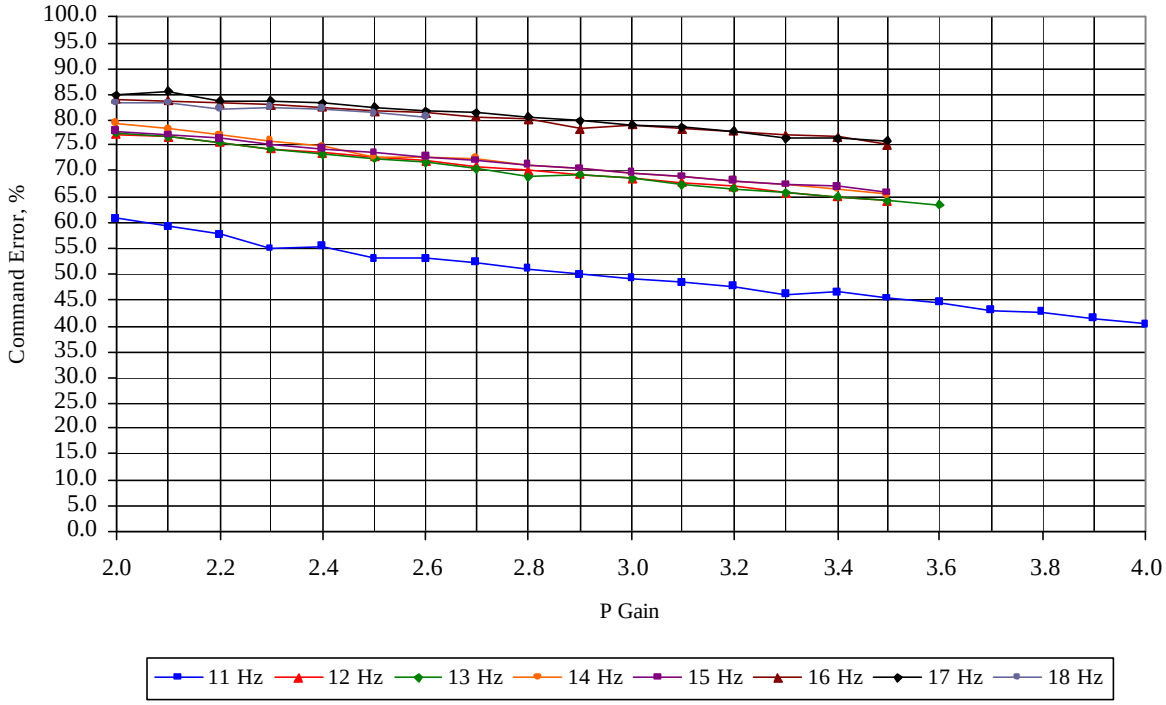

Figure 9.13 Command Error (peak) vs. P-gain (K_P) Tuning for 11.0 to 18.0 Hz.

From Figure 9.14 the valley command error also increased as the frequency increased. Also we noticed that the error decreased almost linearly with K_P and the error decreased more slowly than for the lower frequencies (1 to 10 Hz). Moreover, we noticed that some frequencies are grouped together. The lowest peak command error is 50% for 11.0 Hz at K_P = 4.0. The highest peak command error is 93% for 16, 17 and 18 Hz at K_P = 2.0. The valley command error is greater than the peak command error. We recommend that these tests are run for higher K_P than we did. We only did the tests until some instability was showing on the system.

For tracking the waveform we used the scope that comes with TestStarAP controller software. Using the scope we can see how K_P changed the waveform. We only are going to show the graphs for the following frequencies: 1 Hz, 5Hz, 10Hz, 15 Hz and 18 Hz.

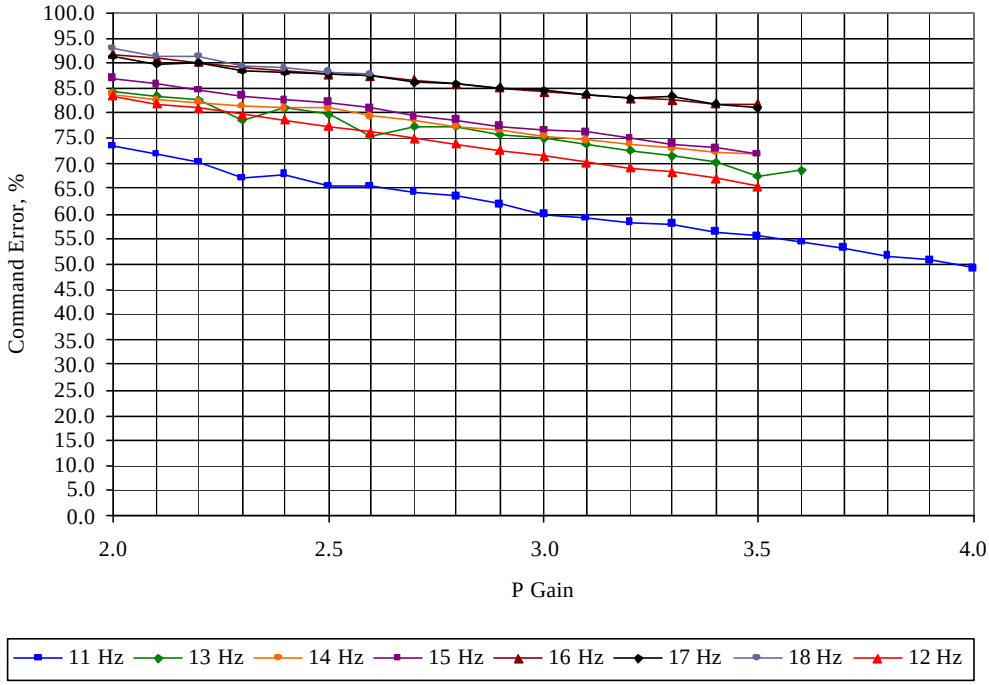

Figure 9.14 Command Error (valley) vs. P-gain (K_P) Tuning for 11.0 to 18.0 Hz.

Figure 9.15 shows the effect of K_P on the 1.0 Hz sinusoidal waveform. Figure 9.16 shows the effect of K_P on the 5.0 Hz sinusoidal waveform. Figure 9.17 shows the effect of K_P on the 10.0 Hz sinusoidal waveform. Figure 9.18 shows the effect of K_P on the 15.0 Hz sinusoidal waveform. Figure 9.19 shows the effect of K_P on the 18.0 Hz sinusoidal waveform. It can be seen that as we increase the K_P the feedback signal (blue curve) tracks the command signal (red curve) more closely. Figure 9.15 illustrates that the value of K_P that best tracks the command signal for 1.0 Hz is $K_P = 6.0$. At the same value of $K_P = 6.0$ at 5.0 Hz, the feedback signal tracks the amplitudes of the waveform more closely but the K_P does not correct the phase lag showing on Figure 9.16. Figures 9.17, 9.18 and 9.19 show that the values of $K_P = 2.0$ to 3.0 for these frequencies do not correct the command error nor the phase lag. Further tests are needed to find the right values.

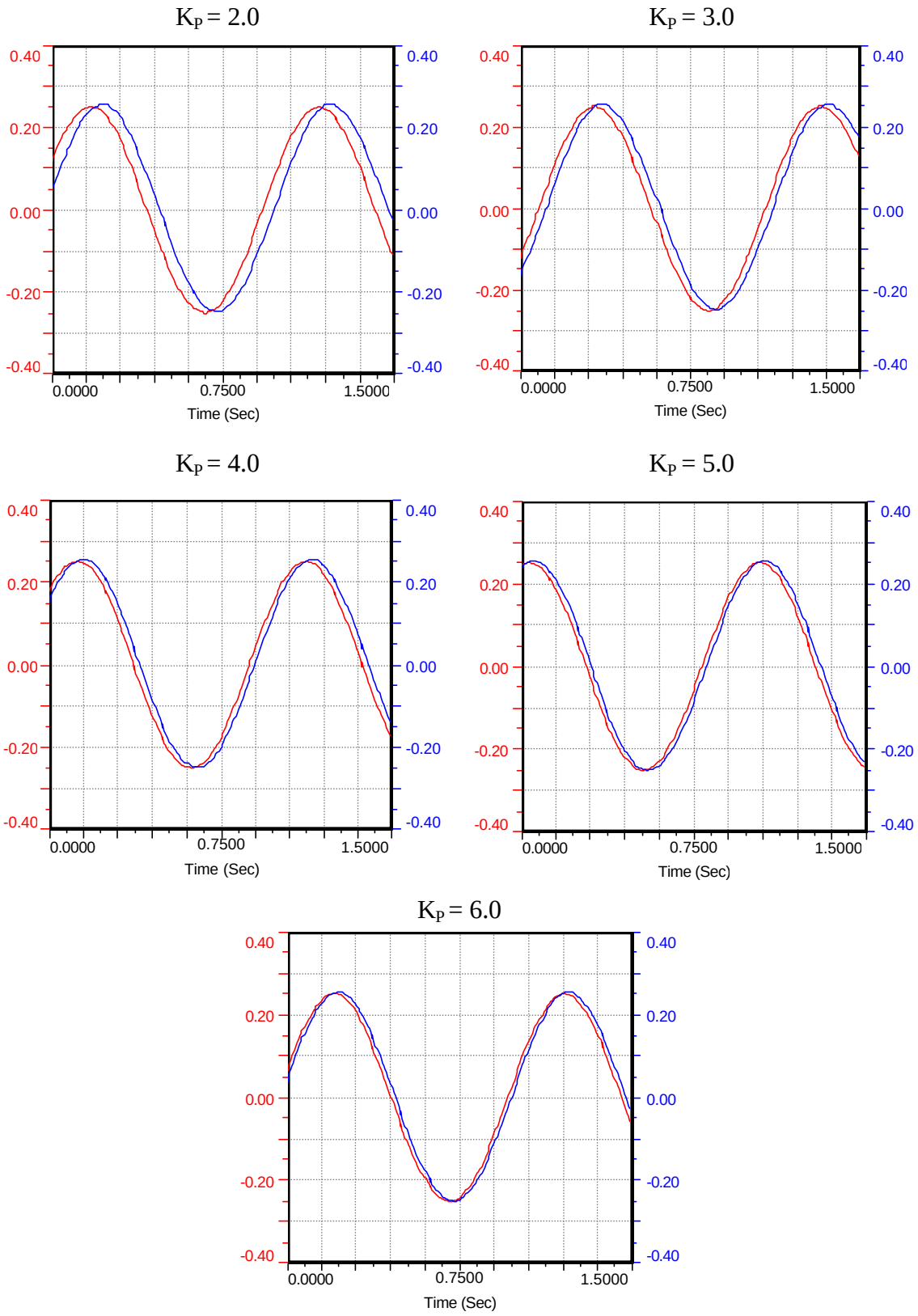

Figure 9.15 Effect of K_P on 1.0 Hz Sinusoidal Waveform.

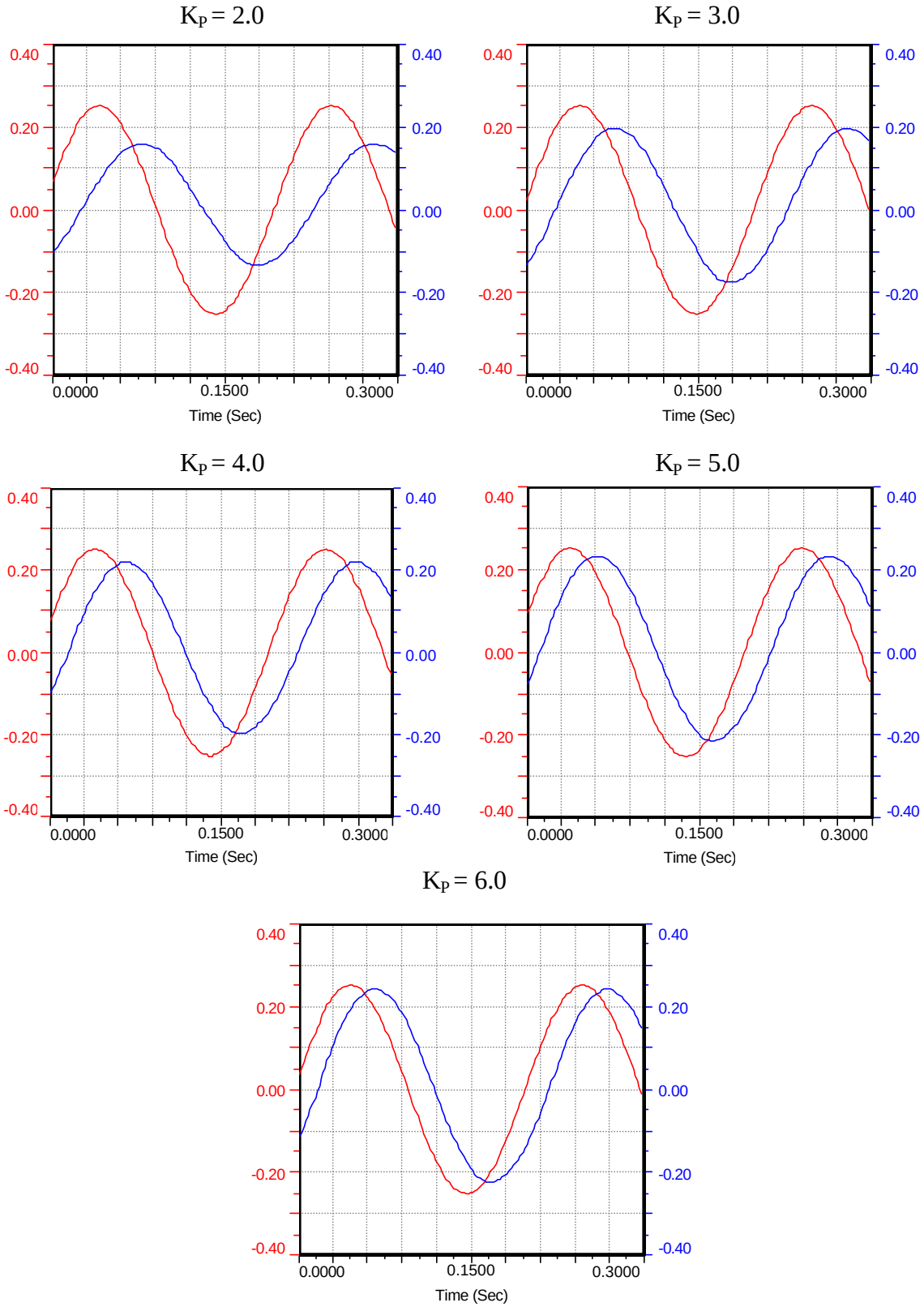

Figure 9.16 Effect of K_P on 5.0 Hz Sinusoidal Waveform.

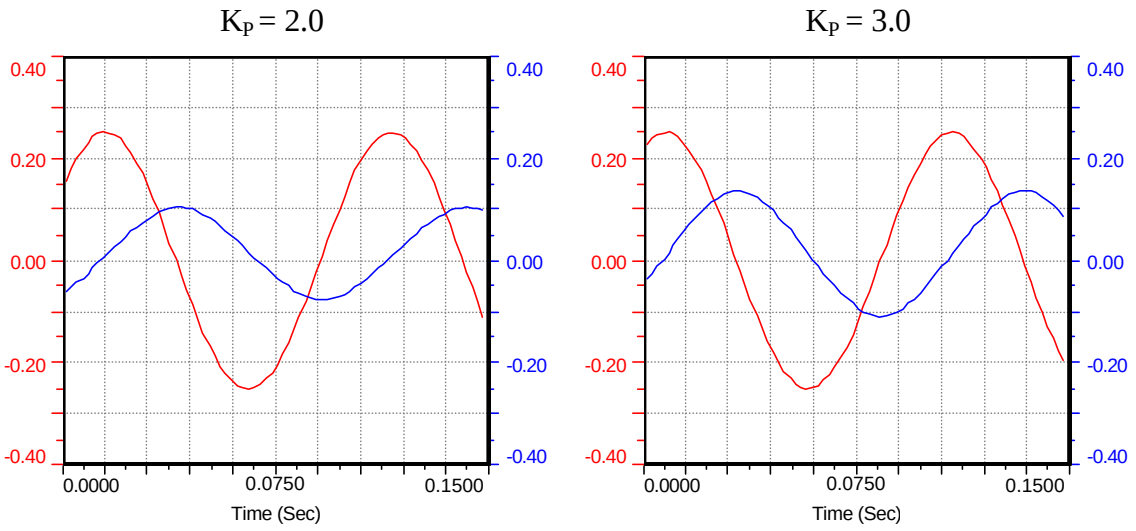

Figure 9.17 Effect of K_P on 10.0 Hz Sinusoidal Waveform.

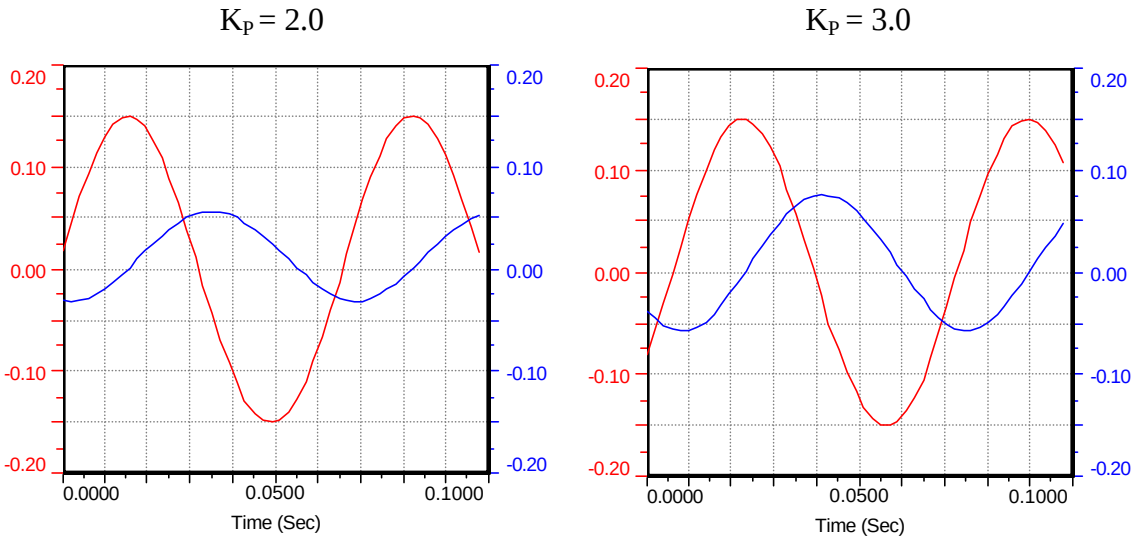

Figure 9.18 Effect of K_P on 15.0 Hz Sinusoidal Waveform.

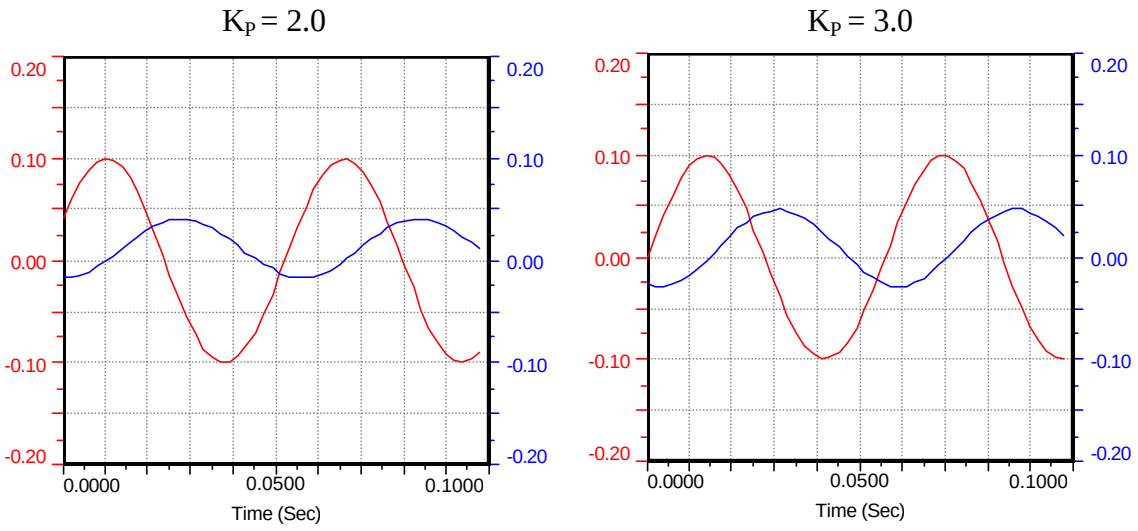

Figure 9.19 Effect of K_P on 18.0 Hz Sinusoidal Waveform.

9.5.2. CHECKING FOR ROTATIONAL MODES OF VIBRATION

From this test series shake table resonances could be found, such as for rocking or rotational mode of vibration, by finding appropriate locations and orientations of measuring devices, such as accelerometers [3]. Figure 9.20 illustrates this concept.

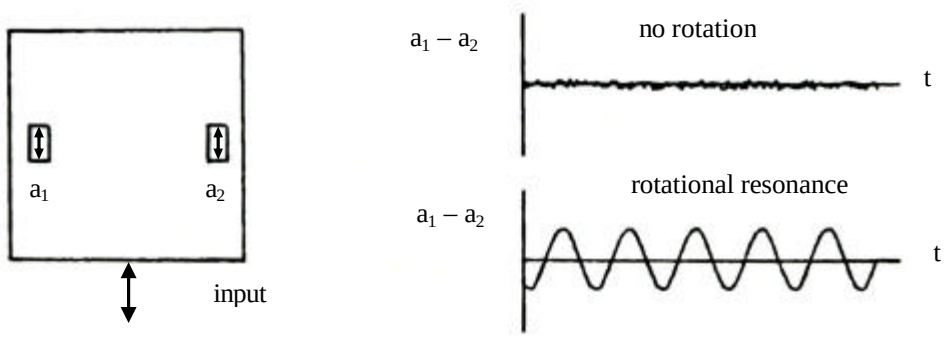

Figure 9.20 Shake Table Rotational Modes [3].

For our system we used accelerometers as our measuring device and positioned them in different locations, as illustrated in Figure 9.21.

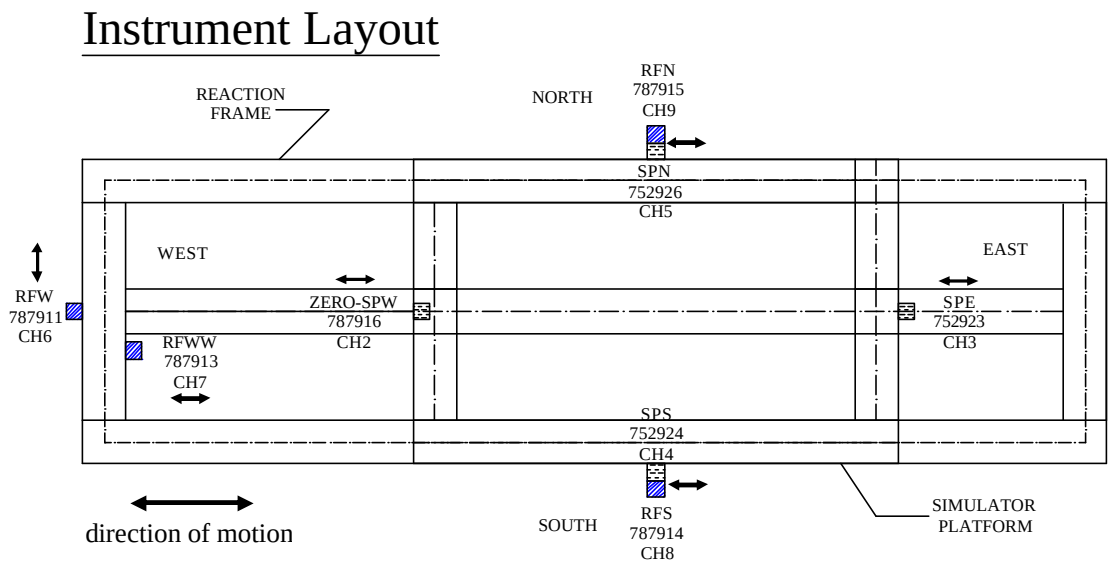

Figure 9.21 Accelerometers Layout.

Mills [3] specifies that these modes should be located and identified for future consideration of possible contribution to the response of specific models.

In our case, for the frequencies from 11.0 Hz to 18.0 Hz, we checked (RFN – RFS) for the reaction frame and (SPN – SPS) for the simulator platform. We only are going to show the graphics for the following frequencies: 11.0 Hz, 15.0 Hz, and 17.0 Hz. For the frequency of 11.0 Hz we are going to show how the curves change with changing K_P. For frequencies 15.0 Hz and 17.0 Hz we are going to show the curves for K_P = 3.5, because it is the K_P where the system shows more response.

Figure 9.22 shows that there is no rotation on the reaction frame. It also shows that there is no significant change on the % of Zero-SPW Acceleration with changing K_P. This percent was taken as the ratio of maximum amplitude of RFN-RFS acceleration to

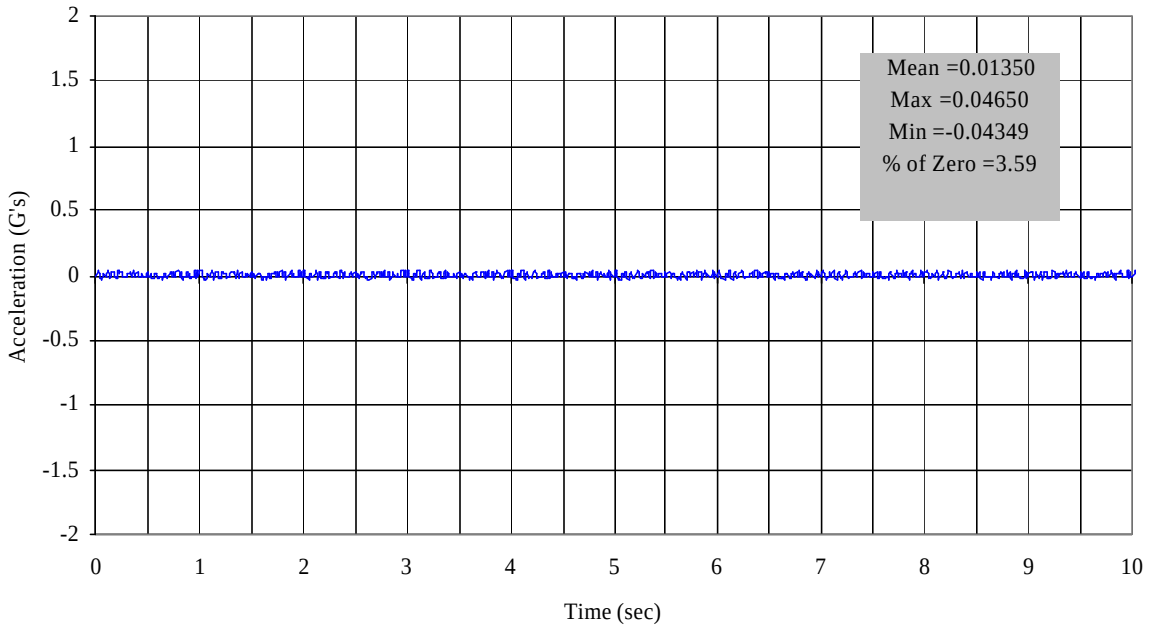

(a) RFN-RFS for 11.0 Hz Sine Wave - $K_P = 2.0$.

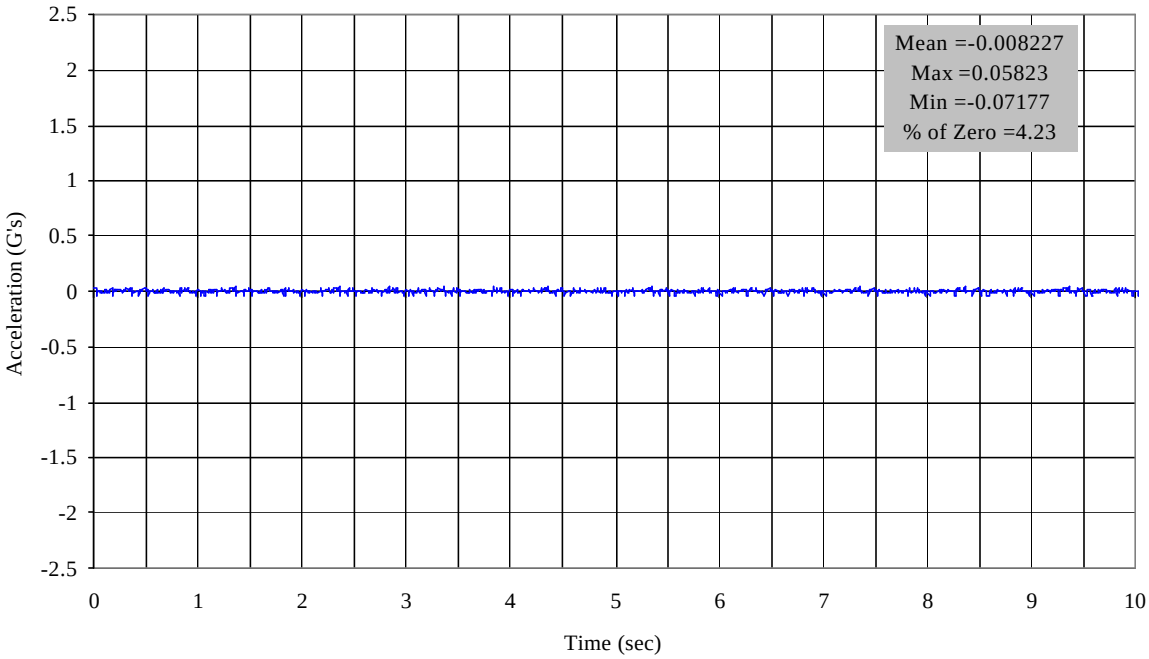

(b) RFN-RFS for 11.0 Hz Sine Wave - $K_P = 2.5$.

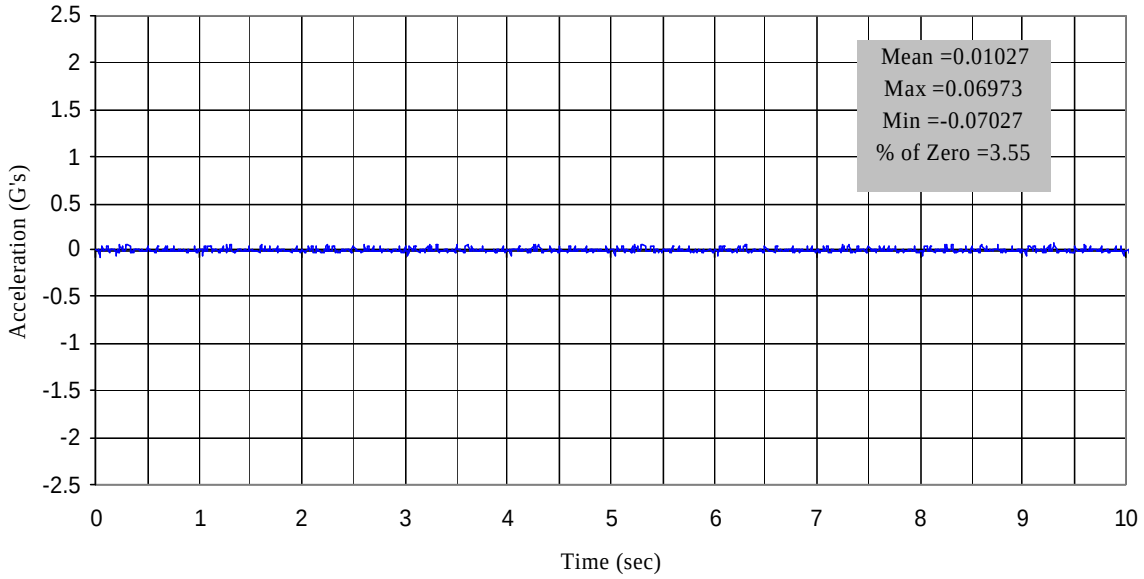

(c) RFN-RFS for 11.0 Hz Sine Wave - K_P = 3.0.

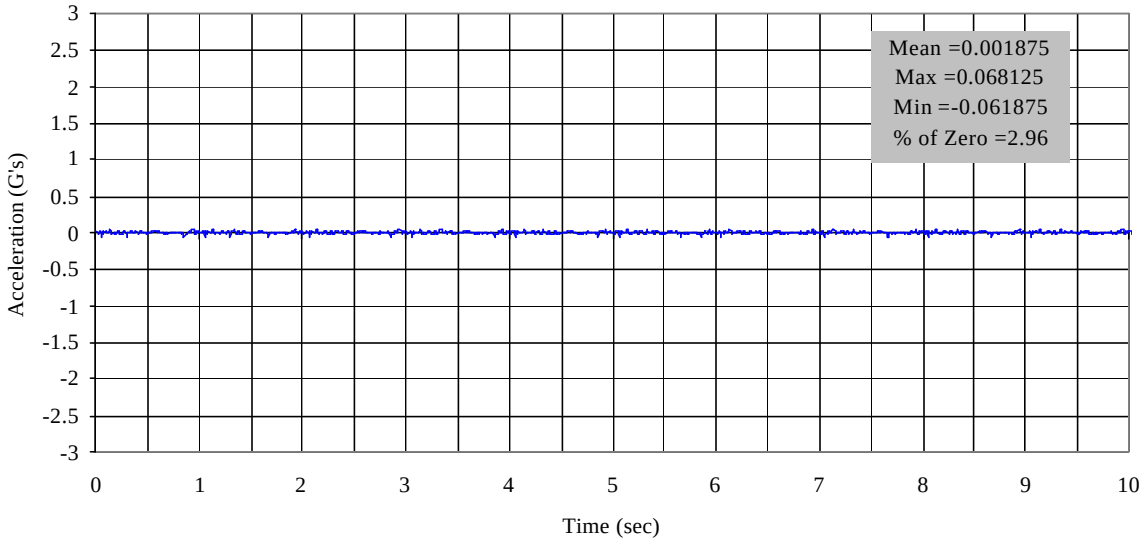

(d) RFN-RFS for 11.0 Hz Sine Wave - K_P = 3.5.

Figure 9.22 Effect of K_P on RFN-RFS for 11.0 Hz.

the maximum amplitude of the Zero-SPW acceleration. This percent went from 2.96 to 4.23.

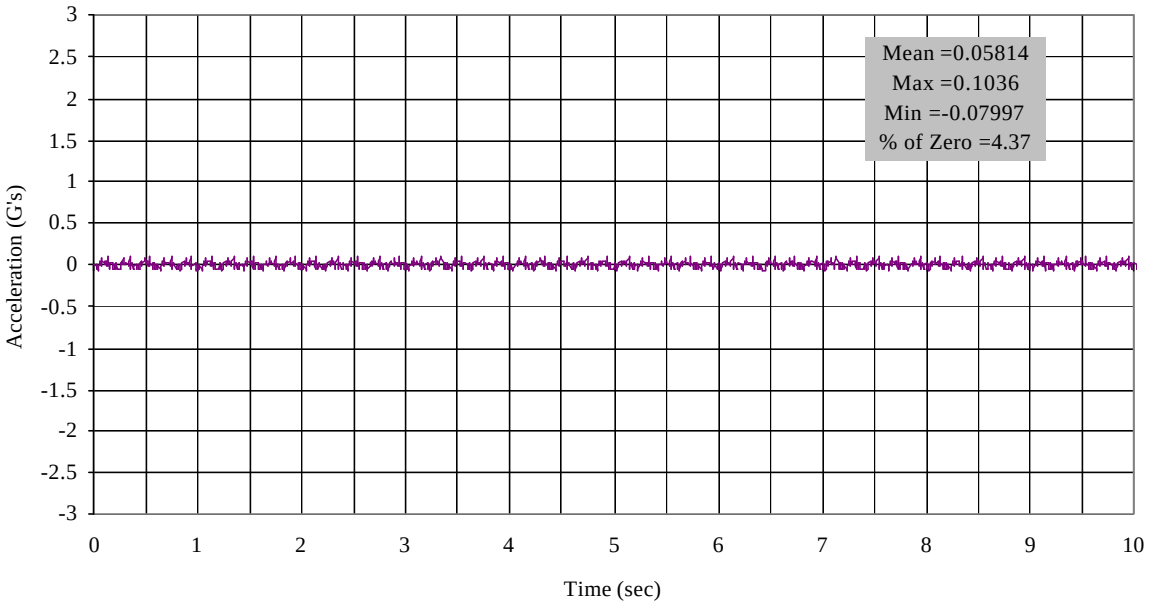

Figure 9.23 RFN-RFS for 15.0 Hz Sine Wave - K_P = 3.5.

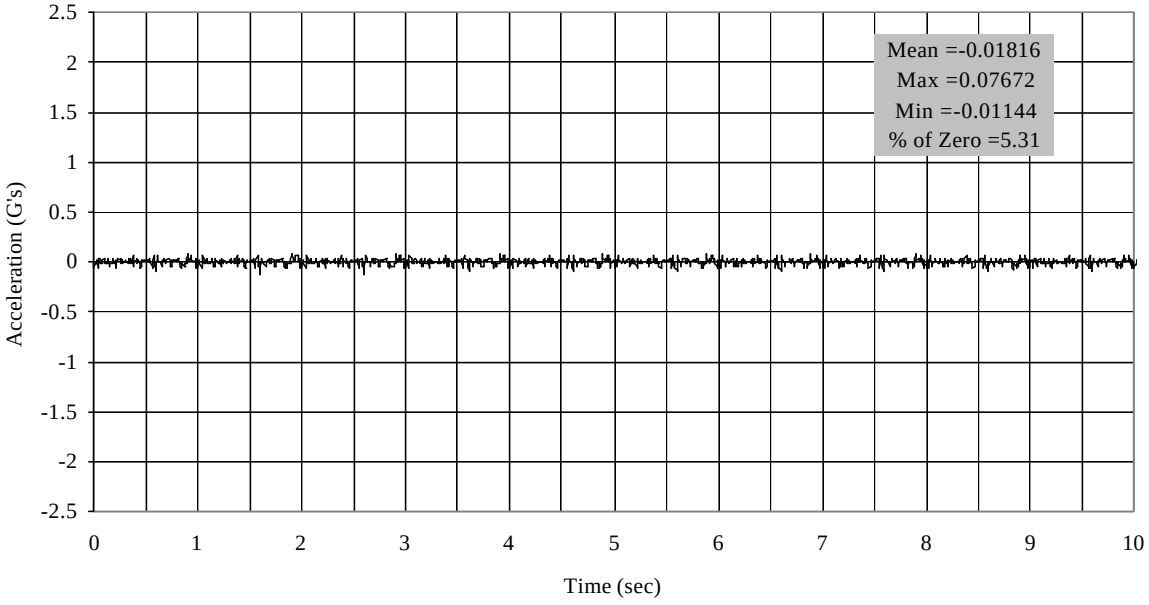

Figure 9.24 RFN-RFS for 17.0 Hz Sine Wave - K_P = 3.5.

Figures 9.23 and 9.24 show RFN-RFS for 15.0 Hz and 17.0 Hz, respectively. These figures show there is no rotation of the reaction frame at these frequencies, also. The % of Zero amplitude went from 4.37 to 5.31. At this point, we conclude there is no rotation of the reaction frame.

Figure 9.25 shows the effect of K_P on SPN –SPS for 11.0 Hz. This figure illustrates there is some rotation on the simulator platform. It also illustrates there is no significant change of % of Zero amplitude with changing K_P until $K_P = 3.5$. This percent went from approximately 20% for $K_P = 2.0$, 2.5 and 3.0 to almost 15% for $K_P = 3.5$.

Figures 9.26 and 9.27 show SPN-SPS for 15.0 Hz and 17.0 Hz, respectively. These figures show there is rotation of the simulator platform at these frequencies, also. The % of Zero amplitude went from almost 14% to 20% for 15.0 Hz and 17.0 Hz, respectively. At this point, we conclude there is some rotation on the simulator platform.

To quantify if this rotation is small or large other measures of behavior have to be considered. Let's consider looking at the curves of the three accelerometers: Zero-SPW, SPN and SPS for the frequencies being studied. Figure 9.28, 9.29 and 9.30 show the curves of the acceleration of the three accelerometers for 11.0 Hz, 15.0 Hz and 17.0 Hz, respectively. The K_P for these curves is 3.5. Looking at the curves it can be seen that the rotation is small and is revealed at the differences in acceleration amplitudes of the three accelerometers. In addition, the rotation shown in one accelerometer, SPS, is larger than the rotation shown in the other accelerometer, SPN. It can be seen from the figures, also, that the acceleration peak and valleys of Zero-SPW and SPN are almost the same. Only SPS shows a significant difference in magnitude of the peaks and valleys compared to Zero-SPW.

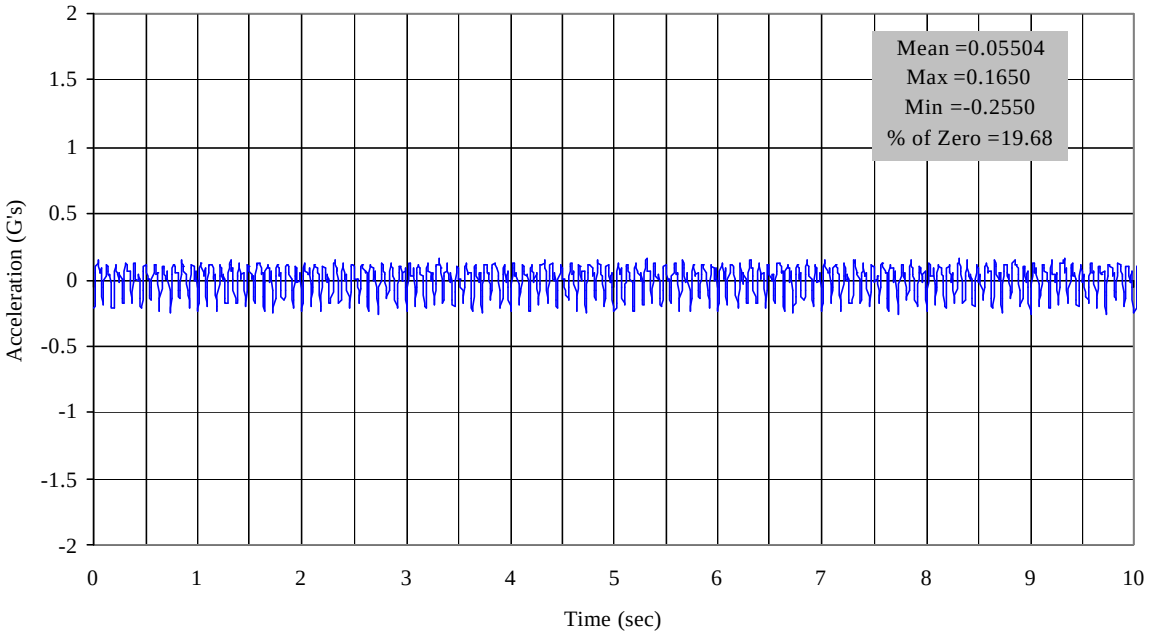

(a) SPN-SPS for 11.0 Hz Sine Wave - K_P = 2.0.

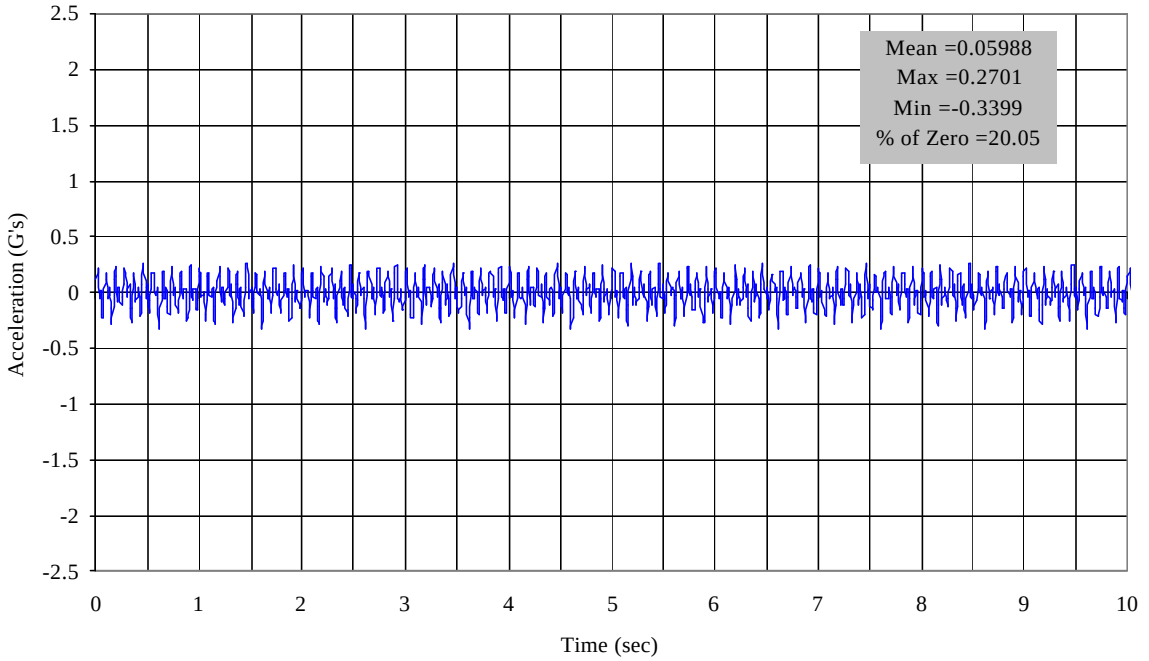

(b) SPN-SPS for 11.0 Hz Sine Wave - K_P = 2.5.

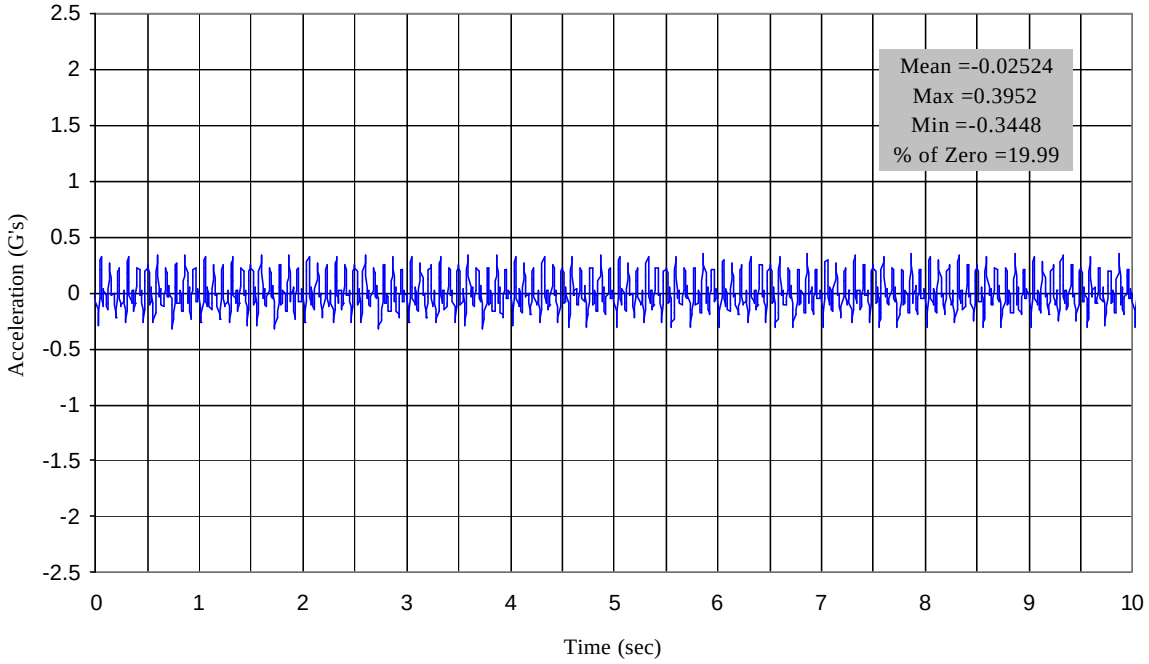

(c) SPN-SPS for 11.0 Hz Sine Wave - K_P = 3.0.

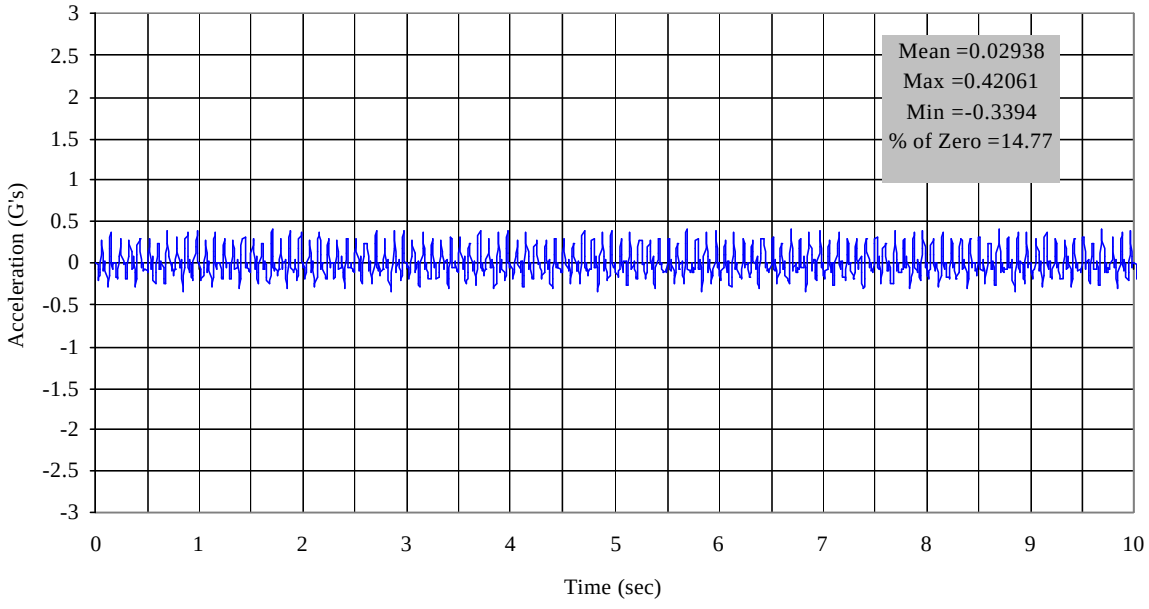

(d) SPN-SPS for 11.0 Hz Sine Wave - K_P = 3.5.

Figure 9.25 Effect of K_P on SPN-SPS for 11.0 Hz.

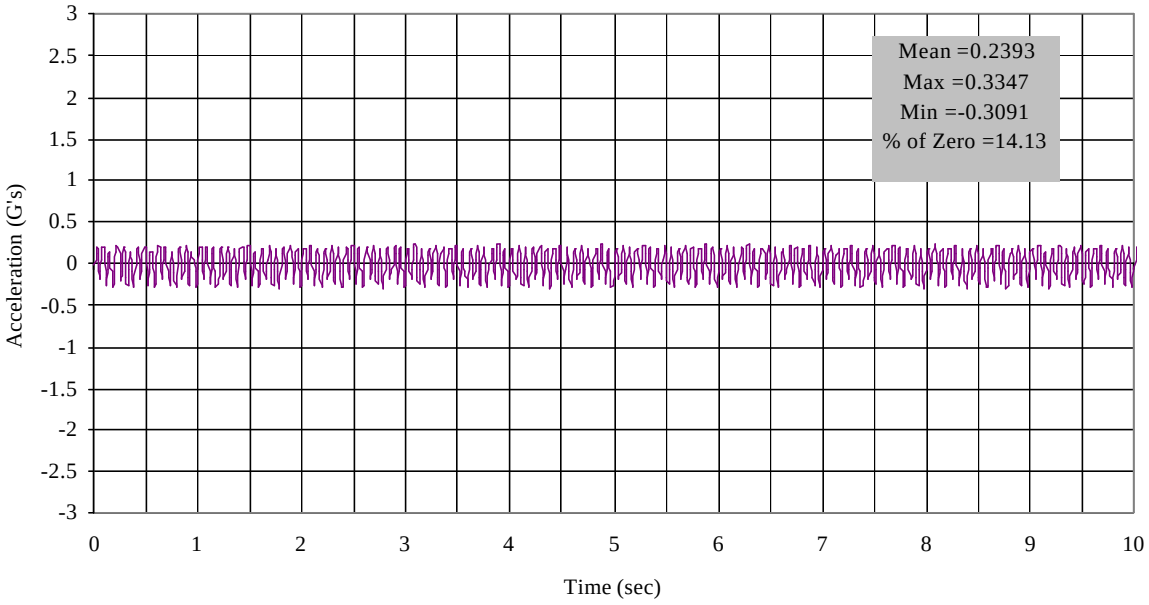

Figure 9.26 SPN-SPS for 15.0 Hz Sine Wave - K_P = 3.5.

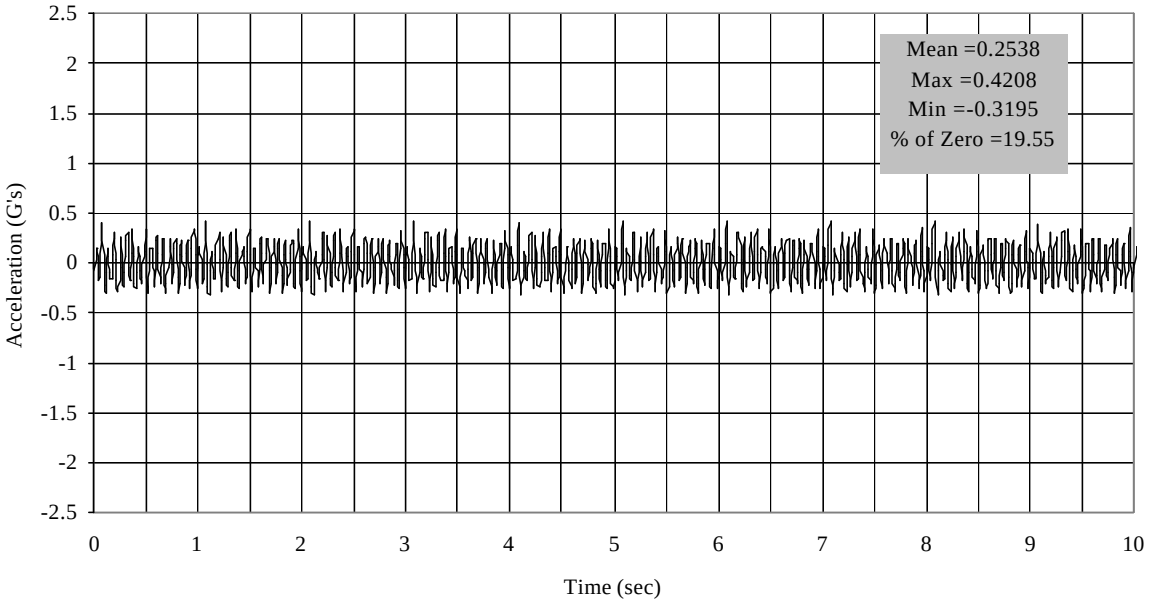

Figure 9.27 SPN-SPS for 17.0 Hz Sine Wave - K_P = 3.5.

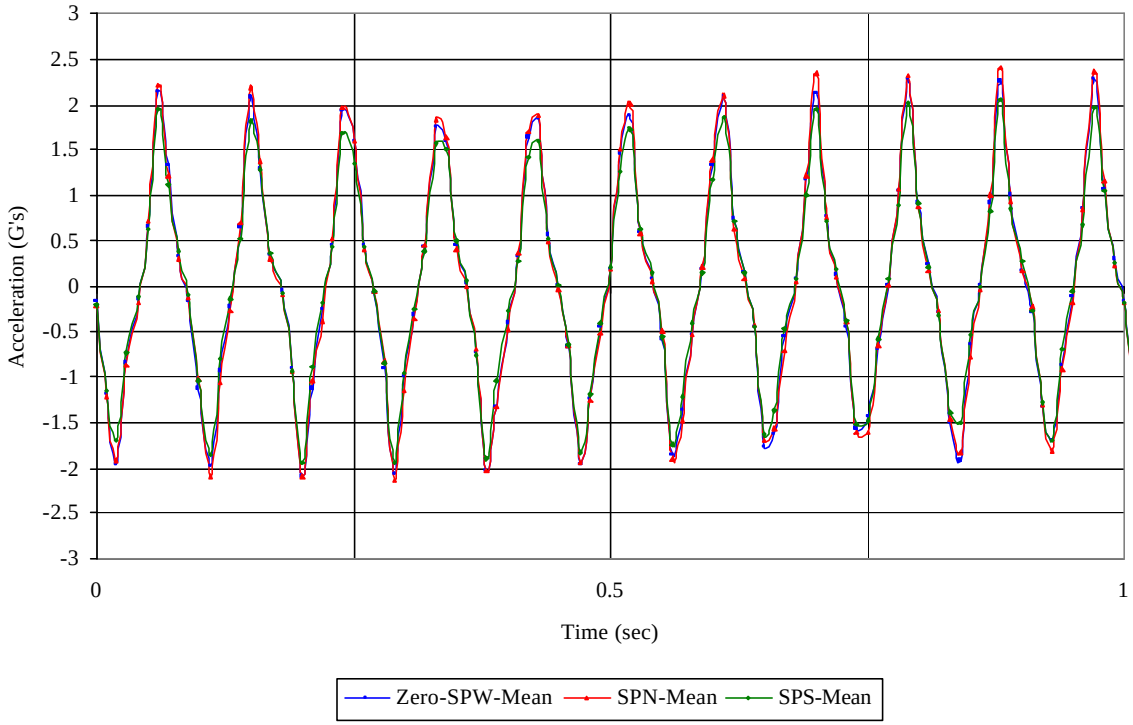

Figure 9.28 Close-Up of 11.0 Hz Sine Wave Acceleration for SPN, SPS and Zero-SPW.

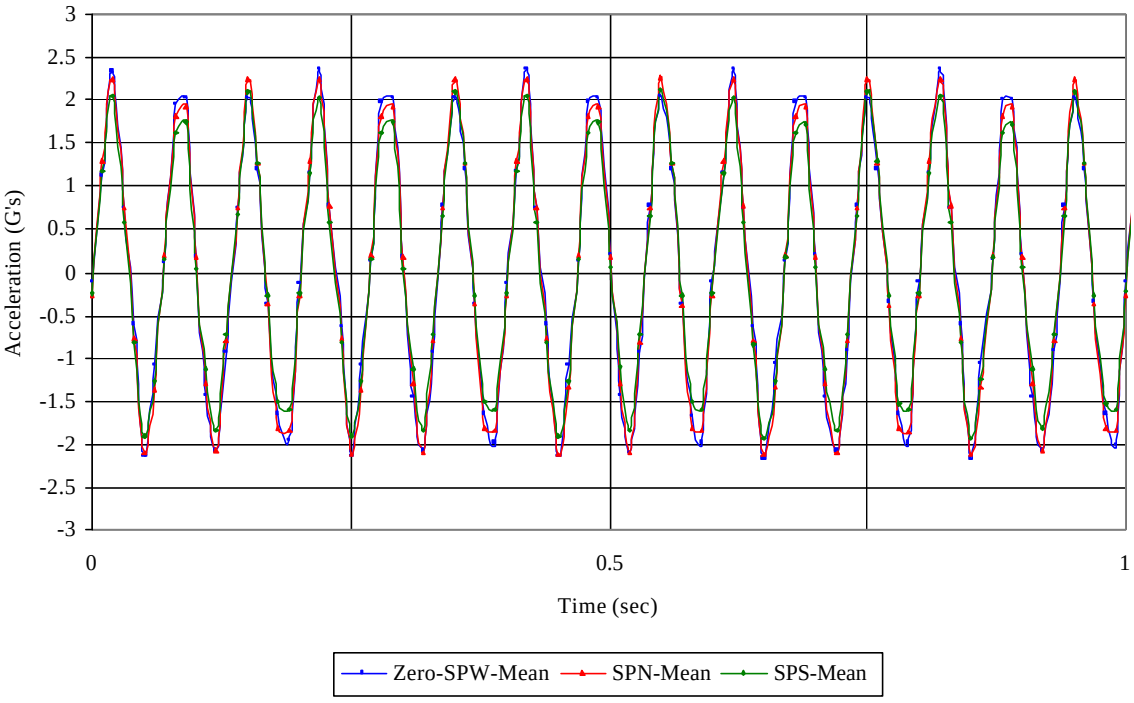

.Figure 9.29 Close-Up of 15.0 Hz Sine Wave Acceleration for SPN, SPS and Zero-SPW.

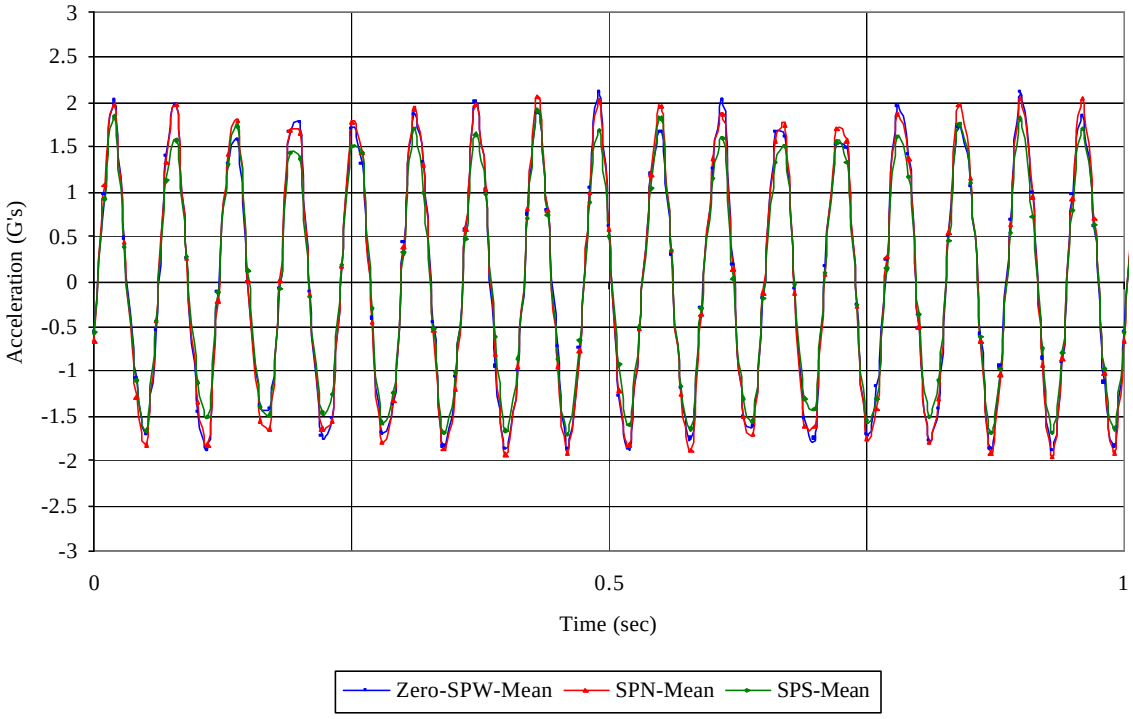

Figure 9.30 Close-Up of 17.0 Hz Sine Wave Acceleration for SPN, SPS and Zero-SPW.

This difference in rotation between the accelerometers may be due to the following factors: mass eccentricity of the platform, a small eccentricity of the actuator applying the displacement or a small misalignment of the linear roller bearings.

The acceleration of SPN is larger than the acceleration of SPS. This behavior is in agreement with the equations of acceleration for a rigid mass that have both translation and rotation, as shown in Figure 9.31. The equations for displacement for point 1 and point 2 are:

$$d_1 = u - \frac{a}{2} * q \tag{9.1}$$

$$d_2 = u + \frac{a}{2} * q \tag{9.2}$$

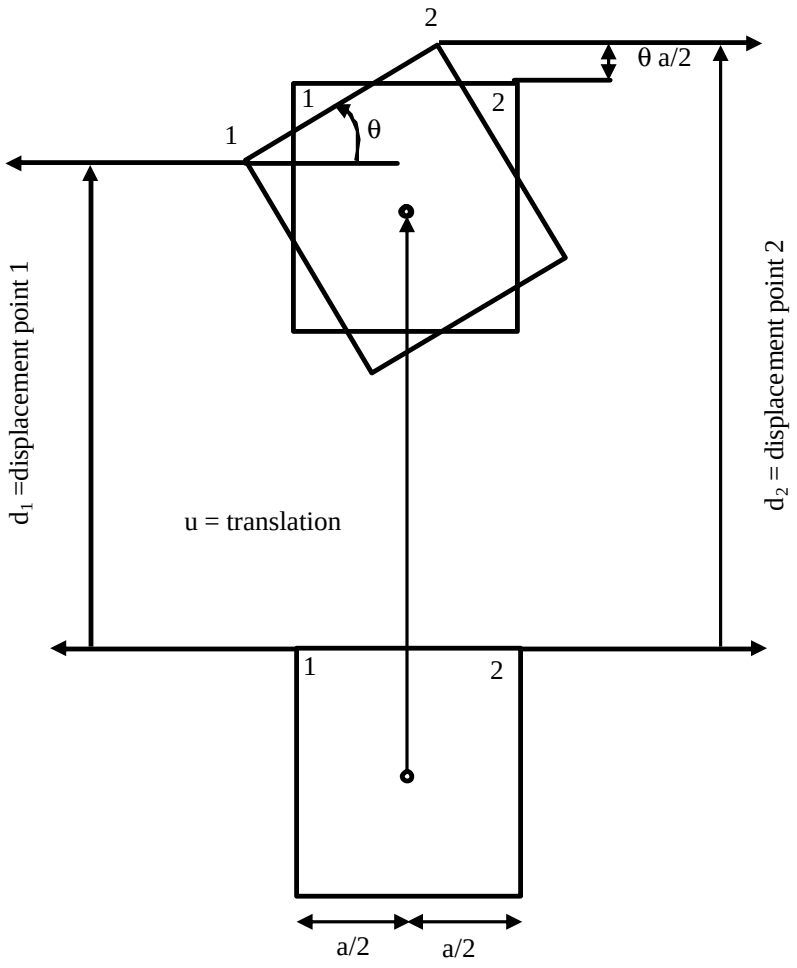

Figure 9.31 Rigid Mass with Translation and Rotation.

Therefore the equations for acceleration for points 1 and 2 are the following:

$$a_1 = \ddot{u} - \frac{a}{2} * \ddot{q} \tag{9.3}$$

$$a_2 = \ddot{u} + \frac{a}{2} * \ddot{q} \tag{9.4}$$

Looking at the equations, SPS is similar to a_1 and SPN is similar to a_2. To obtain the angular acceleration we simply subtract the translational acceleration (Zero-SPW) from

a_1 (SPS) and a_2 (SPN) and divide by 2/a. After following the procedure mentioned above we obtain the following equations:

$$(a_2 - \ddot{u}) * \frac{2}{a} = \ddot{q} \tag{9.5}$$

$$(a_1 - \ddot{u}) * -\frac{2}{a} = \ddot{q} \tag{9.6}$$

Figures 9.32, 9.33 and 9.34 show the curves of angular acceleration using the accelerometer SPN for the following frequencies: 11.0 Hz, 15.0Hz and 17.0 Hz. These curves have a K_P = 3.5. The maximum values of each signal are 3.79, 4.92 to 5.058 rad/sec^2 for sine waves with frequencies 11.0 Hz, 15.0 Hz and 17.0 Hz, respectively. The minimum values of each curve are -3.36, -4.76 to -3.89 rad/sec^2 for 11.0 Hz, 15.0 Hz and 17.0 Hz, respectively.

Figures 9.35, 9.36 and 9.37 show the time variation of the angular acceleration using accelerometer SPS for the following frequencies: 11.0 Hz, 15.0Hz and 17.0 Hz. These curves have a K_P = 3.5. The maximum values of each curve are 4.86, 6.61 to 8.03 rad/sec^2 for 11.0 Hz, 15.0 Hz and 17.0 Hz, respectively. The minimum values are -6.91, -9.52 to -6.44 rad/sec^2 for 11.0 Hz, 15.0 Hz and 17.0 Hz, respectively.

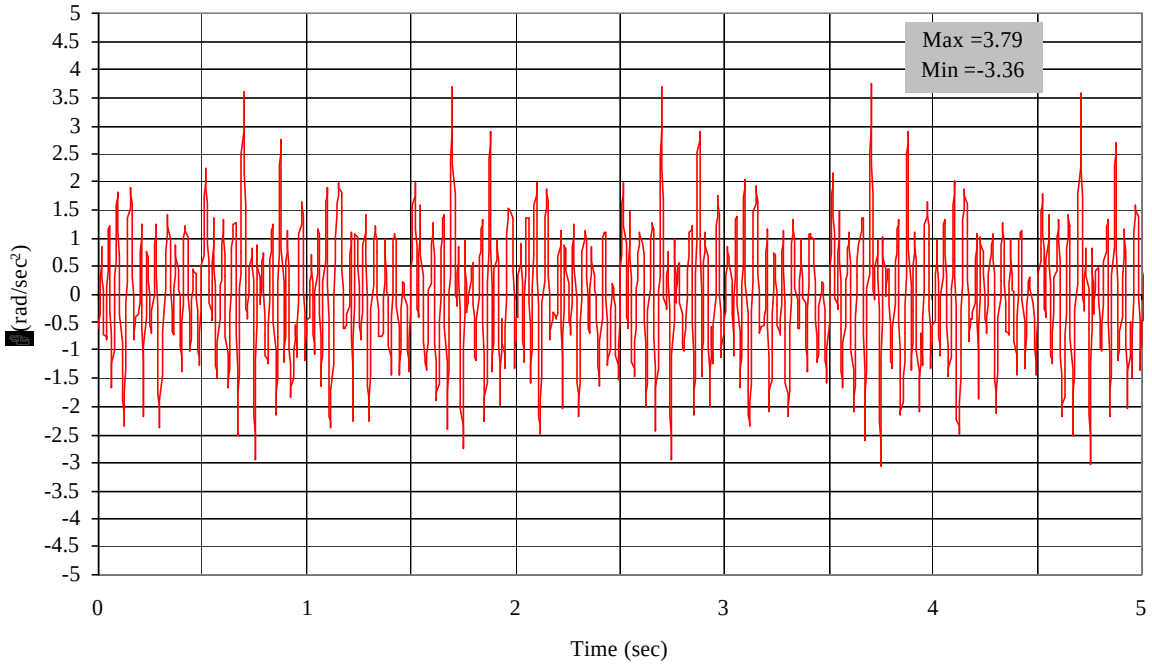

Figure 9.32 (SPN-Zero)-11.0 Hz Sine Wave - K_P = 3.5.

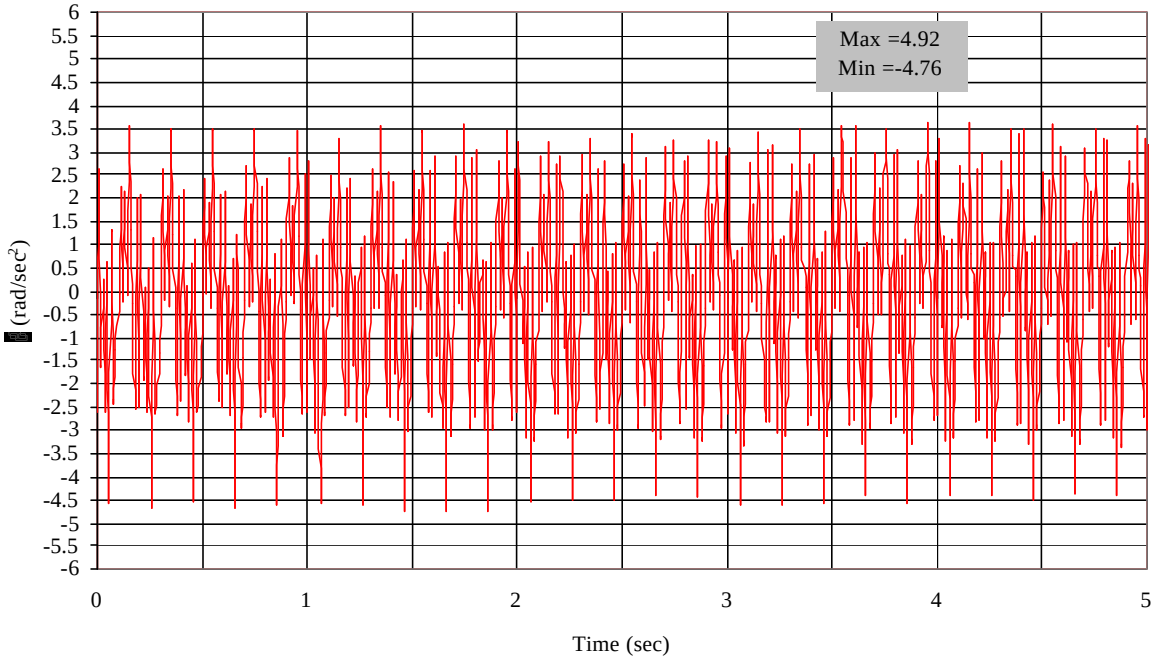

Figure 9.33 (SPN-Zero)-15.0 Hz Sine Wave - K_P = 3.5.

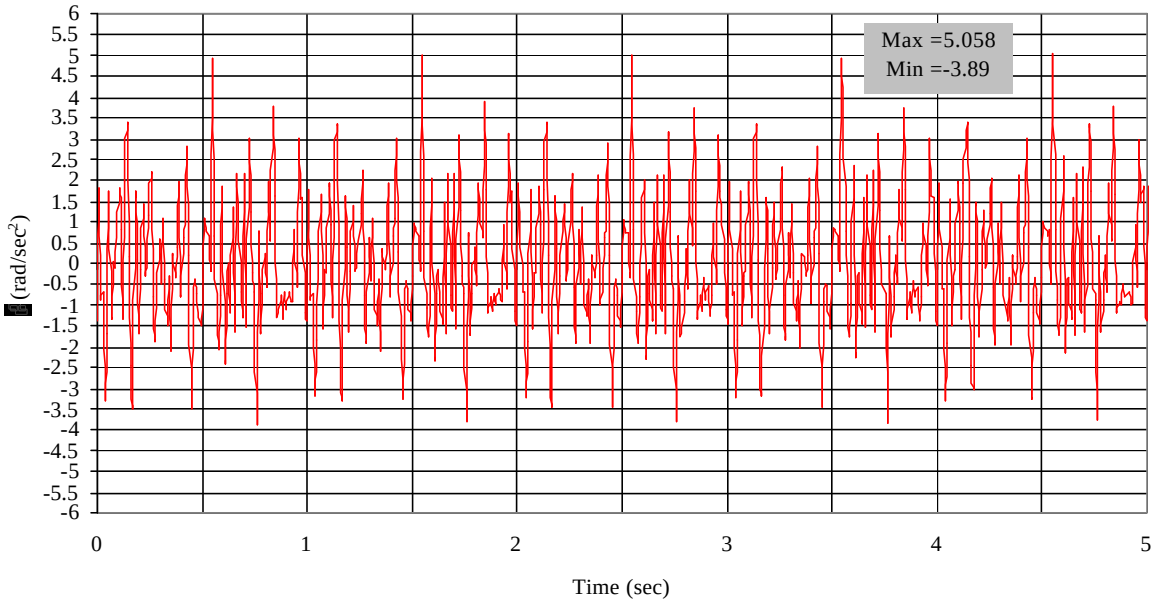

Figure 9.34 (SPN-Zero)-17.0 Hz Sine Wave - K_P = 3.5.

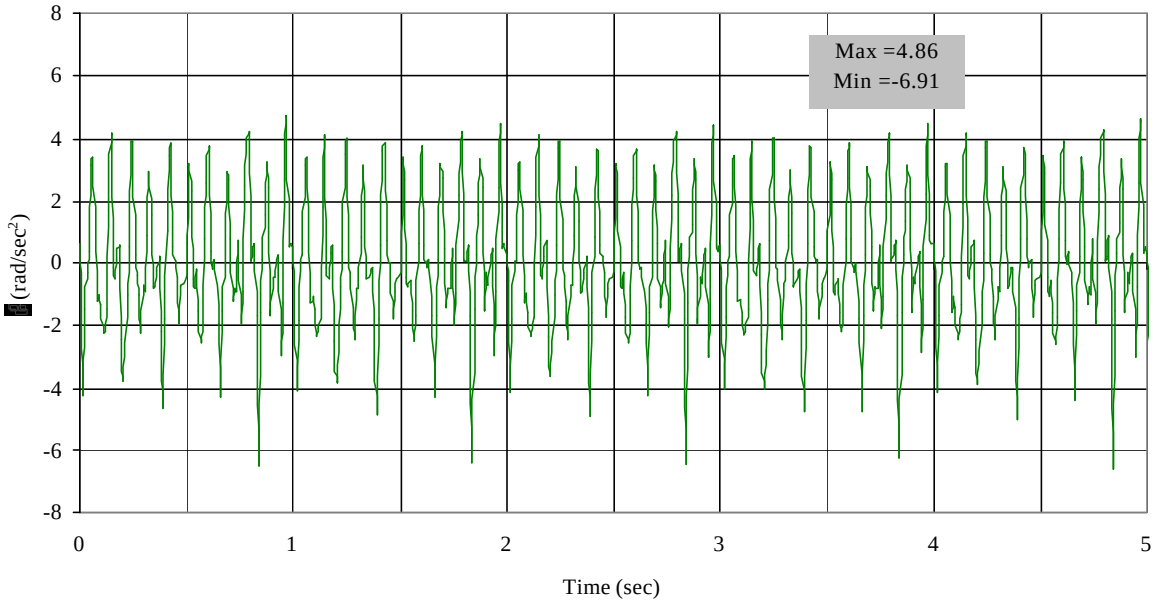

Figure 9.35 (SPS-Zero)-11.0 Hz Sine Wave – K_P = 3.5.

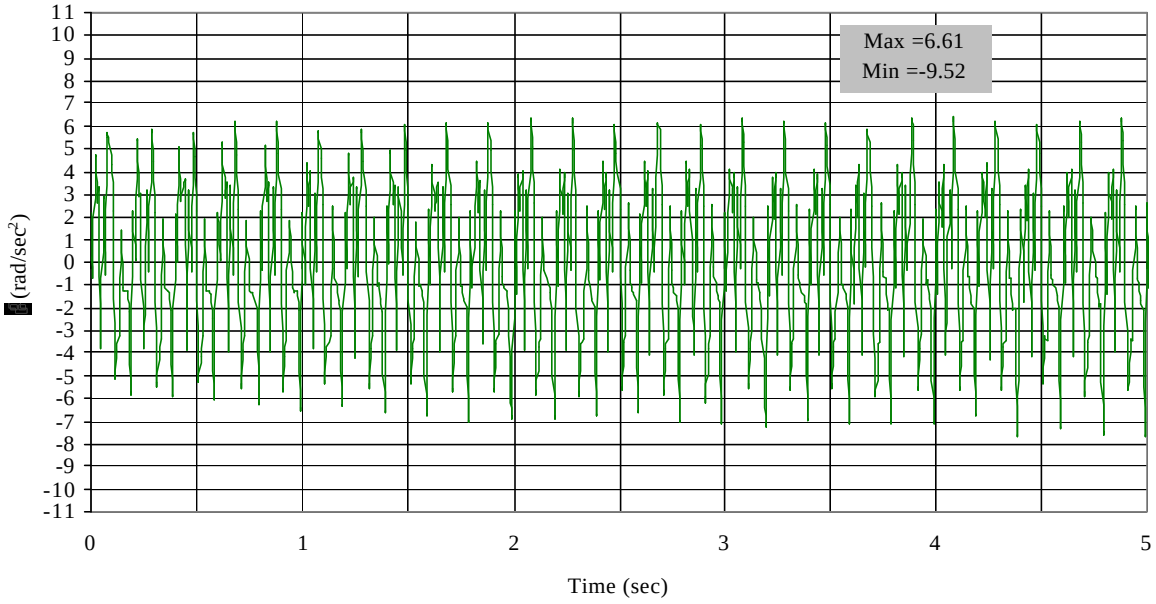

Figure 9.36 (SPS-Zero)-15.0 Hz Sine Wave – K_P = 3.5.

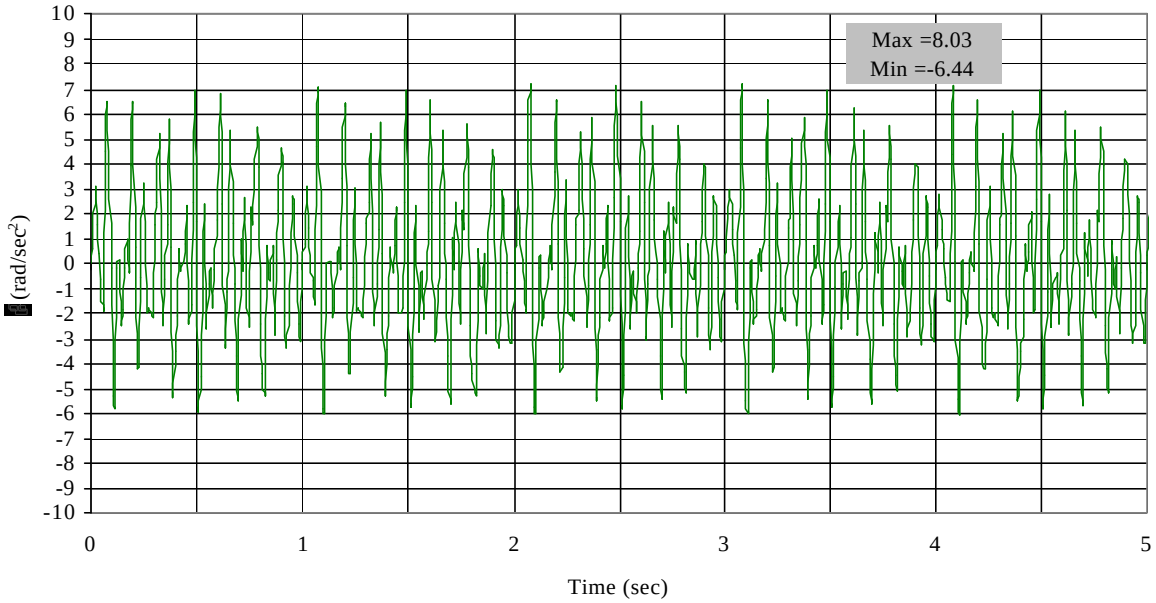

Figure 9.37 (SPS-Zero)-17.0 Hz Sine Wave – K_P = 3.5

9.5.3. COMPARISON IN THE FREQUENCY DOMAIN

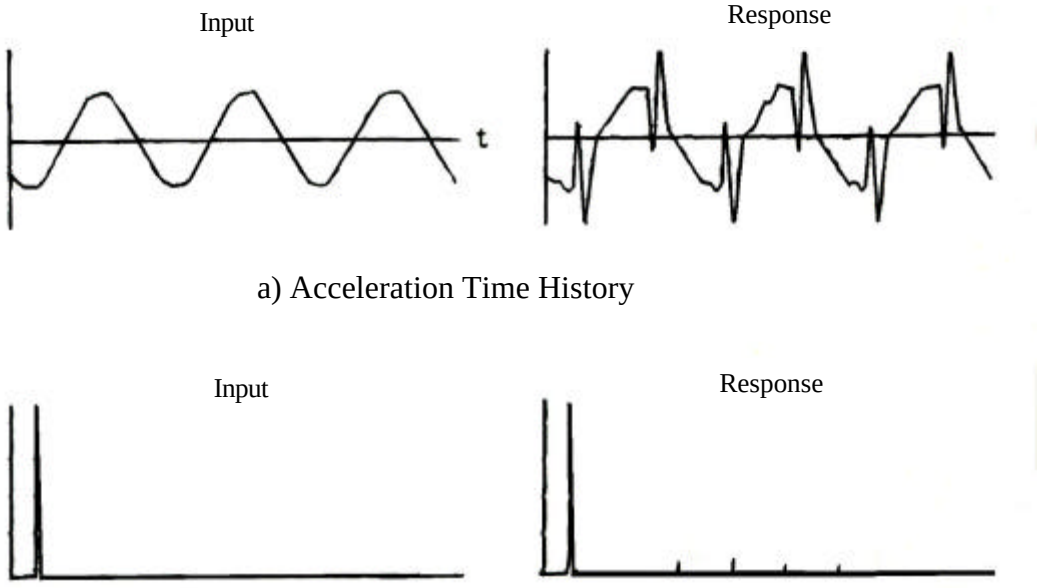

a) Acceleration Time History

b) Fourier Amplitude Spectra

Figure 9.38 Sine Wave Performance [3].

As shown in Figure 9.38, for a single input sine wave the Fourier Spectrum will produce a single frequency impulse. Therefore, any additional frequency components on the Fourier Spectrum of the response signal of the shake table will indicate a distortion of the input signal [3]. The spectrum will also show frequency components that are important to identify, such as the oil column frequency, for further studies using small-scale models on the shaking table.

For this purpose we obtained the Fourier Amplitude Spectrum, of the accelerometer located at Zero- SPW, for all the frequencies studied, from 1 Hz to 18 Hz. For calculating the Fourier Amplitude Spectrum, we used the commercially available program called DADiSP/2002. After studying the results we identified four significant frequency

components: 21 Hz, (24-25) Hz, (27-28) Hz and (30-33) Hz. Figure 9.39 shows the acceleration time history for a 7.0 Hz sine wave and the corresponding Fourier Amplitude Spectrum.

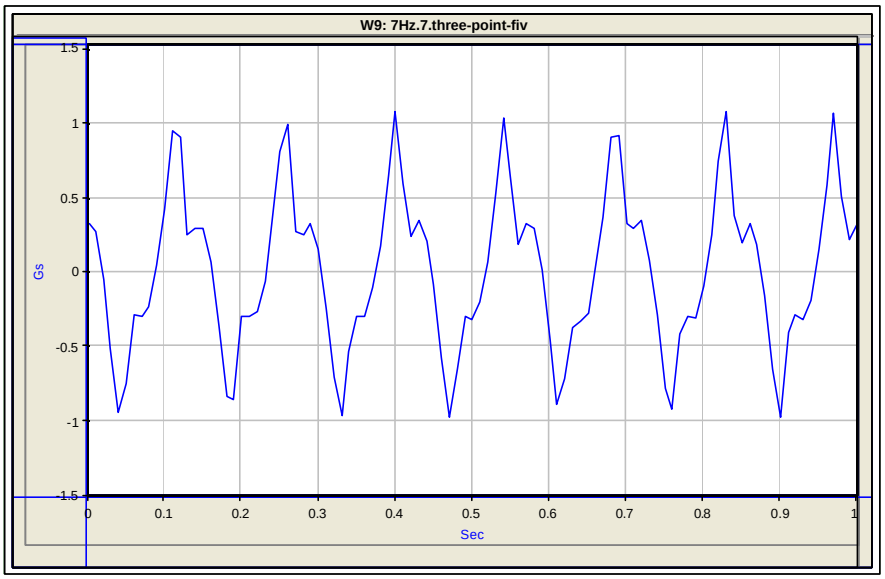

(a) Acceleration Time History of 7.0 Hz Sine Wave – K_P = 3.5.

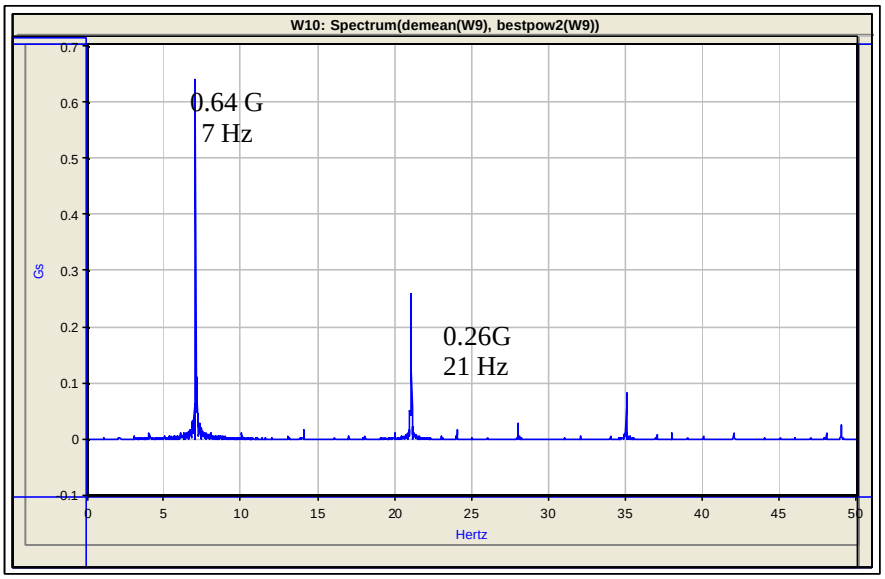

(b) Fourier Amplitude Spectrum for 7.0 Hz Sine Wave –K_P = 3.5.

Figure 9.39 7.0 Hz Sine Wave Performance.

Figure 9.39 (a) shows that the response signal has some distortion. The Fourier Spectrum shown in Figure 9.39 (b) shows a frequency component at 7.0 Hz and at 21.0 Hz. The amplitude of the frequency component of 21.0 Hz is almost 40% of the 7.0 Hz component amplitude.

Figure 9.40 shows the acceleration time history for an 8.0 Hz sine wave and the corresponding Fourier Amplitude Spectrum. As before with the 7.0 Hz sine wave, Figure 9.40 (a) shows that the response signal has some distortion. But the distortion seems to be less than the distortion of the 7.0 Hz sine wave. The Fourier Spectrum shown in Figure 9.40 (b) shows a frequency component at 8.0 Hz and at 24.0 Hz. The amplitude of the frequency component of 24.0 Hz is 56% of the 8.0 Hz component amplitude.

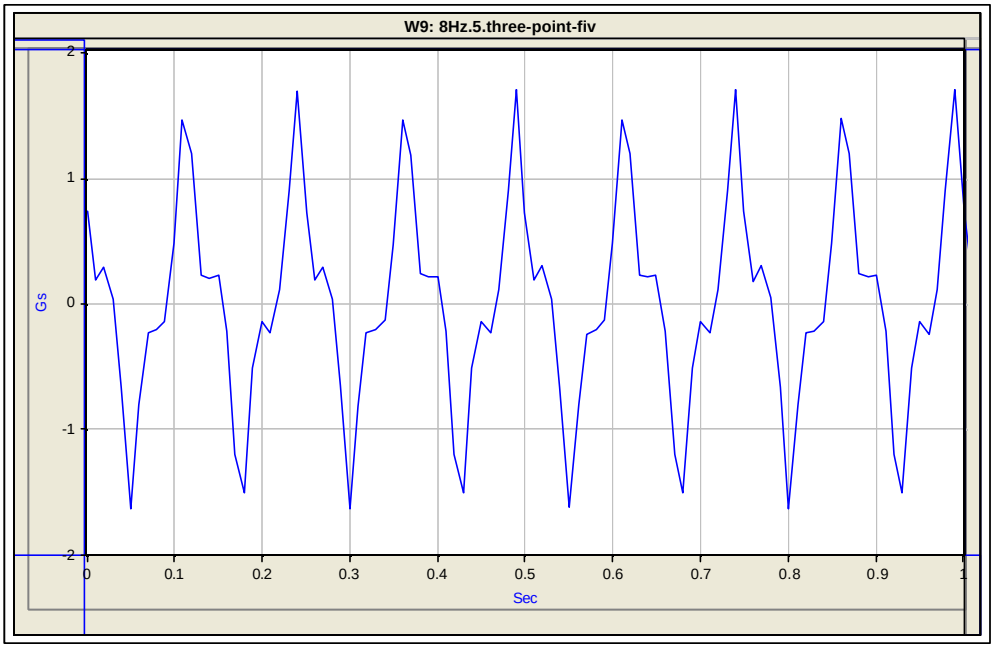

(a) Acceleration Time History of 8.0 Hz Sine Wave – K_P = 3.5.

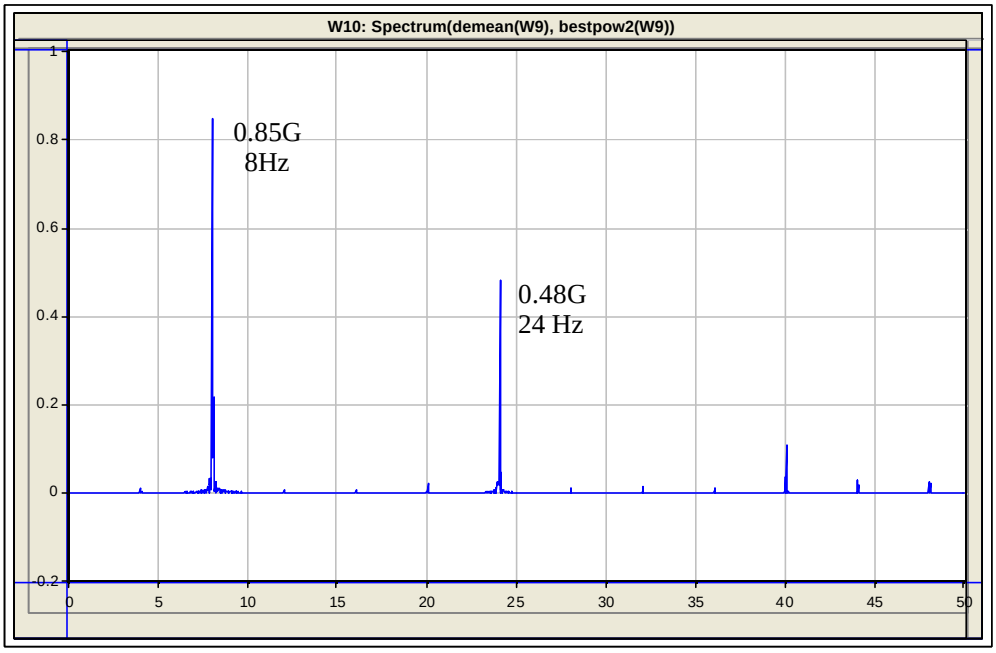

(b) Fourier Amplitude Spectrum for 8.0 Hz Sine Wave – K_P = 3.5.

Figure 9.40 8.0 Hz Sine Wave Performance.

Figure 9.41 shows the acceleration time history for a 9.0 Hz sine wave and the corresponding Fourier Amplitude Spectrum. Figure 9.41 (a) also shows that the response signal have some distortion, but it seems to be decreasing with increasing frequency. The Fourier Spectrum shown in Figure 9.41 (b) shows a frequency component at 9.0 Hz and at 27.0 Hz. The amplitude of the frequency component of 27.0 Hz is 36% of the 9.0 Hz component amplitude.

Finally, Figure 9.42 shows the acceleration time history for an 11.0 Hz sine wave and the corresponding Fourier Amplitude Spectrum. Here also Figure 9.42 (a) indicates that the response signal has some distortion. The Fourier Spectrum shown in Figure 9.42 (b) shows a frequency component at 11.0 Hz and at 33.0 Hz. The amplitude of the frequency component of 33.0 Hz is 28% of the 11.0 Hz component amplitude.

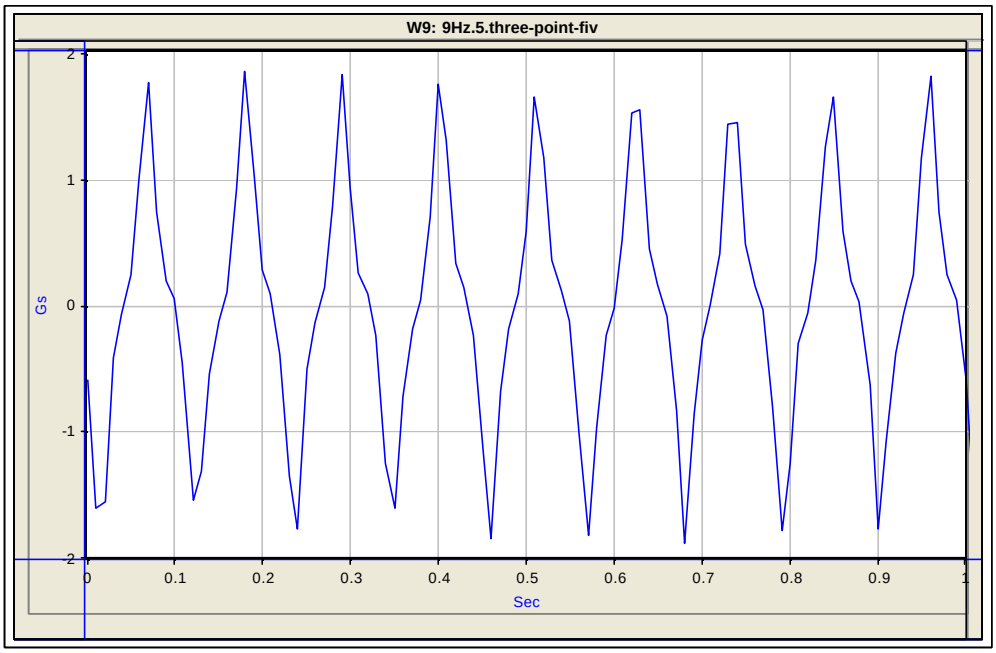

(a) Acceleration Time History of 9.0 Hz Sine Wave – K_P = 3.5.

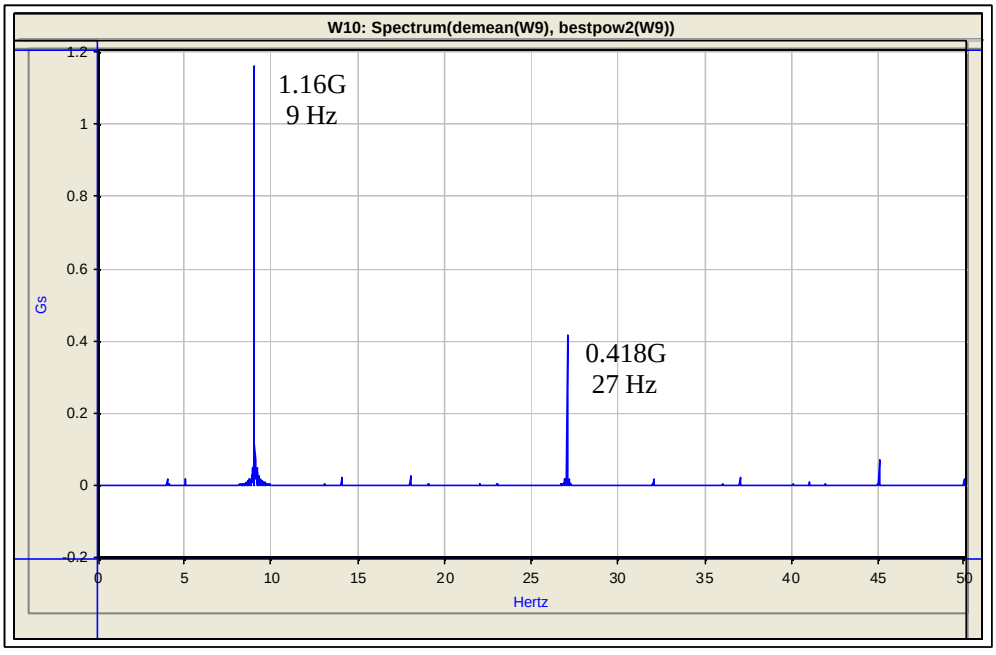

(b) Fourier Amplitude Spectrum for 9.0 Hz Sine Wave – K_P = 3.5.

Figure 9.41 9.0 Hz Sine Wave Performance.

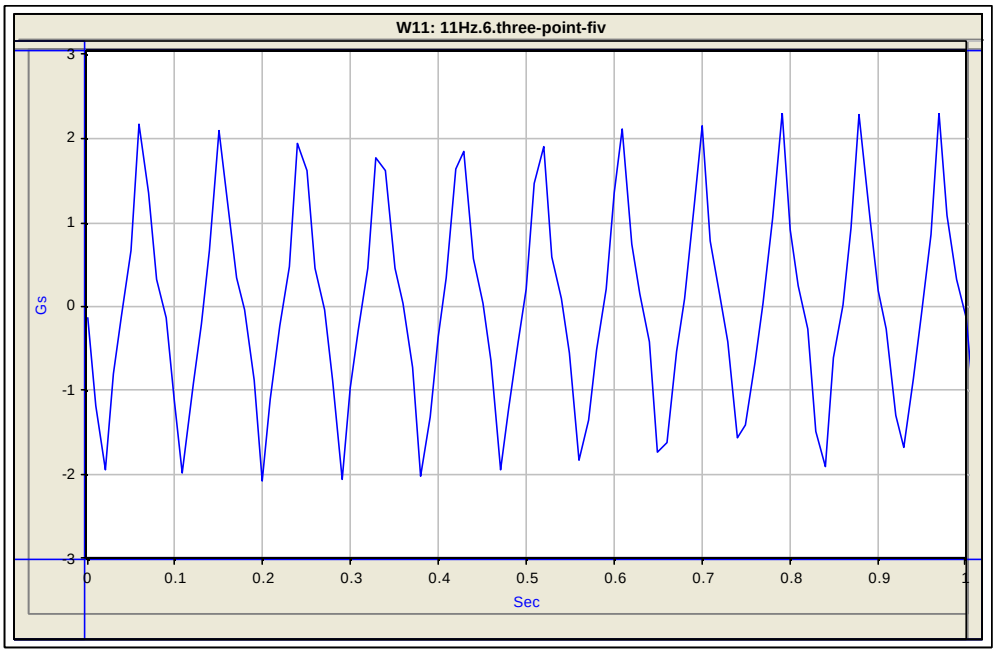

(a) Acceleration Time History of 11.0 Hz Sine Wave – K_P = 3.5.

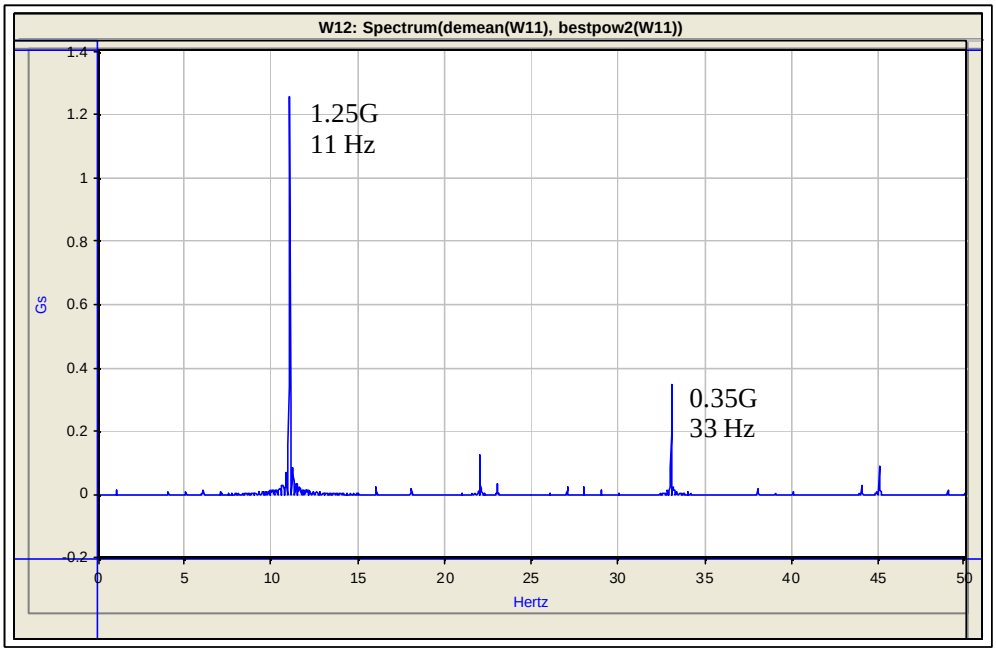

(b) Fourier Amplitude Spectrum for 11.0 Hz Sine Wave – K_P = 3.5.

Figure 9.42 11.0 Hz Sine Wave Performance.

Of the four frequency components encountered at the Fourier Amplitude Spectrum of the frequencies studied, we have identified the oil column frequency at a frequency ranging from 30.0 Hz to 33.0 Hz. The oil column frequency changes with the bulk modulus, as discussed in Chapter 7, and the bulk modulus varies the temperature. The operating temperature of the HPS unit is 125°F (51.67°C). However, the temperature ranges from 90°F (32.2°C) when the HPS unit is cool, to 140°F (60°C) where the HPS shuts down. Further studies are needed to identify the other frequency components.

The behavior for the frequencies from 13.0 Hz to 18.0 Hz was different compared to the behavior of the lower frequencies. When we calculated the Fourier Amplitude Spectrum for these frequencies, only the frequency component of the input signal appeared on the spectrum. No other frequency components showed on the Fourier Amplitude Spectrum. The Fourier Amplitude Spectrum in Figure 9.43 (b) confirms this behavior for the acceleration time history for a 17.0 Hz sine wave.

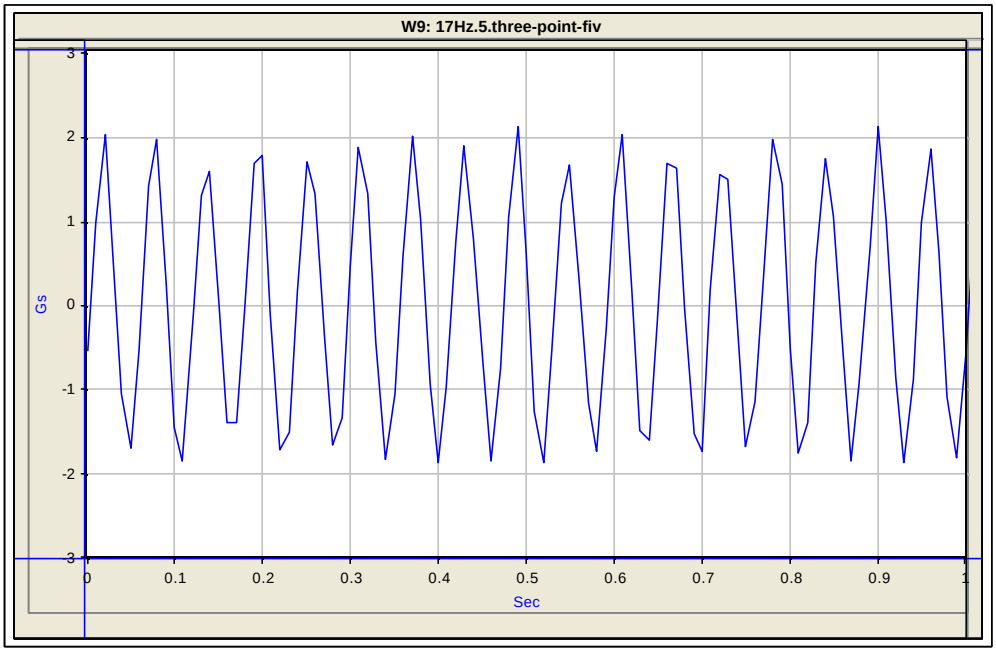

(a) Acceleration Time History of 17.0 Hz Sine Wave – K_P = 3.5.

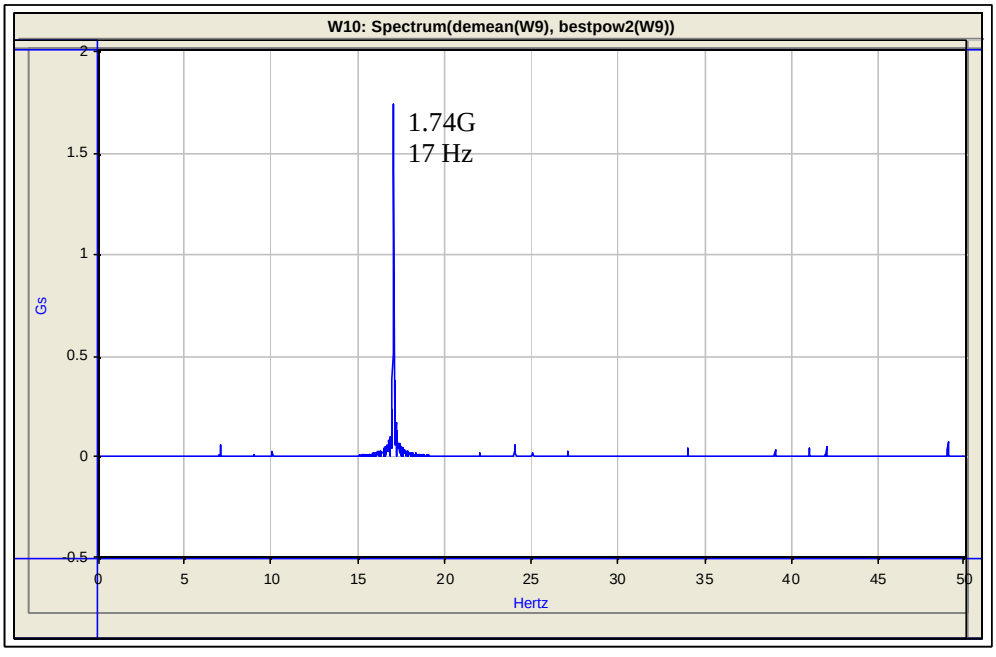

b) Fourier Amplitude Spectrum for 17.0 Hz Sine Wave – K_P = 3.5.

Figure 9.43 17.0 Hz Sine Wave Performance